anti-c-*myc* antibodies (BD Pharmingen, San Diego, CA), or mouse anti-beta-actin antibodies (Santa Cruz Biotechnology, Santa Cruz, CA) and were then incubated with the appropriate horseradish peroxidase (HRP)-conjugated secondary antibodies. Immunocomplexes were visualized with SuperSignal West Femto substrate (Thermo Scientific, Rockford, IL) and detected using an LAS-4000 Mini image analyzer (GE Healthcare, Buckinghamshire, United Kingdom).

Detection of antibodies against EHcV. To detect anti-EHcV antibodies in horse sera, we subjected lysates prepared from 293FT cells expressing EHcVc, which is an N-terminally FLAG-tagged and C-terminally HA-tagged EHcV core protein (a positive reference), or cells transfected with an empty plasmid (a negative reference) to Western blotting, as described above. The resulting PVDF membranes were incubated with Blocking One solution (Nacalai Tesque) for blocking at room temperature for 30 min and then incubated with 1,000-fold-diluted horse serum in 10-fold-diluted Blocking One. Mouse anti-FLAG or rabbit anti-EHcV core antibody was used as a positive serum control. The resulting membrane was incubated with an HRP-conjugated antibody to mouse, rabbit, or horse IgG (Abcam, Cambridge, UK) at room temperature for 1 h. Protein bands with a molecular mass of 28 kDa were detected in the positive reference, but not in the negative reference, using positive serum or an antibody to the FLAG epitope tag or EHcV core protein. The rabbit polyclonal antibody against the EHcV core protein was generated by immunization using peptides of the residues from 2 to 15, GNKSKNQKPQPQRG (Scrum Inc., Tokyo, Japan).

Pulldown assay for SPP binding. Human embryonic kidney 293FT cells expressing EHcVc or HCVc with or without SPP-D219A were harvested at 18 h posttransfection, washed with cold PBS, suspended in 100 μl of the lysis buffer, and centrifuged at 14,000 ×g for 5 min at 4°C. Twenty microliters of the lysate was mixed with 20 μl of 2× SDS sample buffer. The remaining lysate was adjusted to 250 μl with the lysis buffer and incubated for 2 h at 4°C after the addition of 20 μl of His-Select nickel affinity gel (Sigma) equilibrated 50% (vol/vol) with lysis buffer. The nickel beads that included SPP-wt or SPP-D219K were washed five times with 500 μl of lysis buffer by centrifugation at 5, 000 × *g* for 1 min at 4°C and then suspended in 40 μl of 1× SDS sample buffer. After being boiled at 60°C for 20 min, the supernatant was subjected to Western blotting to detect the coprecipitated core proteins.

Immunofluorescence microscopy. Huh7OK1 cells were incubated with fresh DMEM containing Bodipy 558/568 (2 μg/ml; Molecular Probes) for 1 h at 37°C to visualize lipid droplets (LDs). The cells were washed once with prewarmed DMEM and incubated for 30 min at 37°C. The treated cells were then fixed in 4% paraformaldehyde for 30 min at room temperature. After two washes with PBS, the cells were permeabilized with permeabilization buffer containing 0.1% saponin (eBioscience, San Diego, CA) for 30 min at 37°C and blocked with PBS containing 2% FBS (blocking buffer) for 30 min at room temperature. The cells were incubated with an appropriate antibody, as indicated in the figure legends. The cells were washed three times with PBS. The mounted cells were observed with a FluoView FV1000 laser scanning confocal microscope (Olympus, Tokyo, Japan). Nuclei were stained with 4′,6′-diamidino-2-phenylindole (DAPI).

Flotation assay. A flotation assay was carried out according to the method described previously (17). Briefly, 293FT cells expressing EHcVc or EHcVc-mt were cultured on a 10-cm dish. The transfected cells were washed once with cold PBS at 18 h posttransfection and harvested using a cell scraper. The cells were suspended in 1.2 ml of 25 mM Tris-HCl (pH 7.5) containing 150 mM NaCl, 5 mM EDTA, and protease inhibitor cocktail (Merck, Calbiochem) (TNE buffer) and were then homogenized by 10 passes through a 26-gauge needle. Each 0.6-ml aliquot of the homogenates was incubated for 30 min on ice with or without 1% Triton X-100 and was then mixed with 0.4 ml of OptiPrep (Axis-Shield, Oslo, Norway). An appropriate concentration of OptiPrep was adjusted with TNE buffer. This mixture was overlaid with 1.2 ml of 30% OptiPrep, 1.2 ml of 25% OptiPrep, and 0.8 ml of 5% OptiPrep, in that order, and was centrifuged at 42,000 rpm for 5 h at 4°C in an SW50.1 rotor (Beckman Coulter, Fullerton, CA). Each fraction, with a volume of 0.4 ml, was collected from the top of the centrifugation tube and was then precipitated by mixing with 4 volumes of cold acetone at −30°C. The resulting pellet was resolved in 50 μl of 1× sample buffer and then subjected to Western blot analysis using a mouse anti-FLAG antibody (Sigma), a rabbit anti-calreticulin antibody (Sigma), and a rabbit anti-caveolin-1 antibody (Sigma). The fractions containing calreticulin in the absence and presence of Triton X-100 were defined as the membrane and detergent-soluble membrane fractions, respectively. In the presence of the detergent, fractions 3 to 5, which contained caveolin-1 but only small amounts of calreticulin, were defined as the detergent-resistant membrane fractions.

Nucleotide sequence accession numbers. The whole sequence of the EHcV strain isolated from serum sample 3 was deposited in GenBank under accession number AB863589. The nucleotide sequences of the partial NS5B-coding regions and 3′ UTRs from samples 5 and 1 were registered as AB921150 and AB921151, respectively.

RESULTS

Detection of the EHcV genome and antibody to EHcV in sera of Japanese-born horses. To clarify whether NPHVs were distributed in Japan, we collected 31 horse serum samples and examined them in order to detect the EHcV genome and antibody to the core protein. We prepared total RNAs from horse sera and screened them using RT-PCR analyses with three sets of PCR primers (NPHV-F1/NPHV-R1, NPHV-F2/NPHV-R2, and NPHV-F3/NPHV-R3) that targeted the NS3-coding region that is relatively conserved among NPHVs. Total RNA prepared from conventional rabbit serum was used as a negative control. PCR products with the expected sizes were found in horse serum samples 1, 3, 25, 26, 27, and 29 to 31 using NPHV-F1/NPHV-R1, in horse serum samples 3 and 5 using NPHV-F2/R2, and in horse serum samples 1, 3, 5, 20, and 25 to 31 using NPHV-F3/R3 (Fig. 1A). The EHcV genome was detected in 11 of 31 (35%) serum samples by RT-PCR (Fig. 1A and B). Copy numbers of the EHcV genome in horse sera varied from 10^4 to 10^9 copies per ml of sera (Fig. 1B). Although a PCR product was slightly amplified from serum sample 19 by PCR using the primer pair NPHV-F1/R1, the copy number of the virus genome in serum sample 19 was estimated to be low, at a level similar to that of the negative control. Thus, we could not determine whether serum sample 19 included a viral genome. We then immunologically surveyed horse sera by Western blotting. Western blotting analyses using horse sera to detect antibodies to the EHcV core protein (Fig. 2) showed that the sera of samples 1, 2, 3, 5, 14, 20, and 25 were immunoreactive to the EHcV core protein (7 positive serum samples of a total of 31 samples; 22.6%). The sera of samples 1, 3, 5, and 20 were PCR positive and seropositive. Serum samples 2 and 14 were PCR negative and seropositive, whereas samples 26 to 31 were PCR positive and seronegative. These results suggest that EHcV has infected Japanese-born domestic horses.

Genetic analysis of EHcV. PCR products corresponding to the 5′ UTR and the open reading frame were segmentally amplified from serum sample 3 by 5′ RACE and RT-PCR, respectively. In the present study, we successfully determined the 3′-terminal sequence downstream of a stop codon using the 3′-RACE method with poly(U) polymerase. We determined the nucleotide sequence of the putative full genome, which was designated JPN3/JAPAN/2013 (GenBank accession number AB863589). The full-length genome of strain JPN3/JAPAN/2013 is composed of 9,355 nucleotides, consisting of the 5′ UTR with a nucleotide length of 389, the 3′ UTR with a nucleotide length of 134, and an open

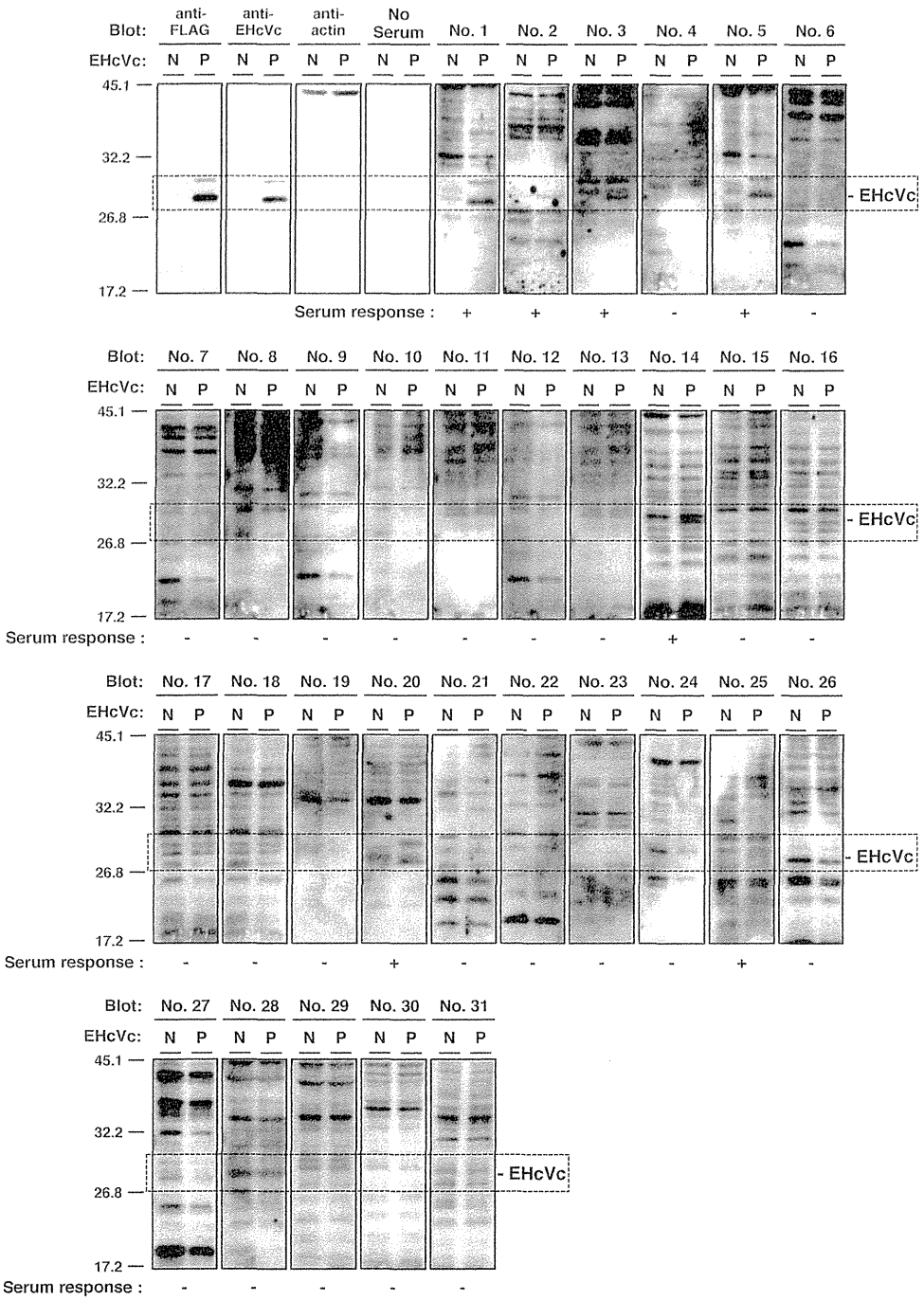

FIG 2 Serological screening of Japanese-born domestic horses. Lysates of 293FT cells transfected with an empty plasmid (a negative reference, N) or the plasmid encoding EHcVc (a positive reference, P) were subjected to Western blotting using serum from each horse. The serum response "+" indicates that the protein band with the same molecular size as the EHcV core protein was specifically detected in the "P" lane, but not in the "N" lane, while the serum response "−" indicates that the protein band with the same molecular size as the EHcV core protein was detected in neither the "P" lane nor the "N" lane. Both antibodies to the FLAG tag and to the EHcV core protein were used as serum positive controls, while protein amounts were standardized with blotting using the antibody to beta-actin. "No serum" indicates the membrane was incubated without primary antibodies but with HRP-conjugated anti-horse IgG antibodies as a background of the secondary antibody.

reading frame with a nucleotide length of 8,832. The open reading frame encodes 2,943 amino acids. Table 2 summarizes the amino acid homology of the JPN3/JAPAN/2013 polyprotein with the polyproteins of the other EHcV strains. The polyprotein of JPN3/JAPAN/2013 shared more than 94% homology with the other EHcV polyproteins and exhibited the highest homology, 97.8%, with NPHV-H10-094 (GenBank accession number JQ434007), which was isolated from a horse in the United States (8). The NS3- and NS5B-coding regions of the EHcV strains were phylogenetically analyzed by the neighbor-joining method. The phylogenetic

TABLE 2 Amino acid sequence homologies of the polyproteins

	Non-primate hepaciviruses					
	H10-094 (JQ434007)	B10-022 (JQ434004)	NZP1 (JQ434001)	AAK-2011 (JF44991)	H3-011 (JQ434008)	A6-066 (JQ434003)
JPN3/JAPAN/2013 (AB863589)	97.8[a]	96.7	95.7	95.7	95.6	95.3

	Non-primate hepaciviruses		HCV			
	G1-073 (JQ434002)	F8-068 (JQ434005)	HCV1a (NC004102)	HCV1b (AB779562)	JFH1 (AB047639)	GBV-B (NC001655)
JPN3/JAPAN/2013 (AB863589)	94.9	94.1	46.5	45.6	44.5	28.9

	Non-primate hepaciviruses		
	JPN3/JAPAN/2013 (AB863589)	AAK-2011 (JF44991)	GBV-B (NC001655)
HCV1a (NC004102)	46.1	46.0	33.3

[a], percent identity.

trees of the NS3 (Fig. 3A) and NS5B regions (Fig. 3B) showed that JPN3/JAPAN/2013 was included in the clade comprising the U.S. strains NPHV-H10-094 (GenBank accession number JQ434007) and B10-022 (GenBank accession number JQ434004).

Putative RNA secondary structures around the UTRs of EHcV. The 5′-terminal region of JPN3/JAPAN/2013 was compared with those of the EHcV genomes (Fig. 4A). The HCV internal ribosome entry site (IRES)-like structure was embedded in the 5′ UTRs of NPHVs (5, 6). The 5′-UTR region was well conserved among the EHcV strains and showed a mean diversity of approximately 4% among the EHcV strains (Fig. 4A). The 3′-terminal sequence downstream of the (A)-rich region in the EHcV genome had not been reported because the (A)-rich region downstream of the stop codon of EHcV interrupted the reaction in the ordinary 3′-RACE method (5, 6). In the present study, we determined the nucleotide sequences downstream of the (A)-rich region from serum sample 3 (JPN3/JAPAN/2013; GenBank accession number AB863589), sample 5 (JPN5/JAPAN/2015; GenBank accession number AB921150), and sample 1 (JPN1/JAPAN/2015; GenBank accession number AB921151) by the modified 3′-RACE method using poly(U) polymerase, although the region in serum sample 1 was incompletely amplified (Fig. 4B). The regions downstream of the (A)-rich region were conserved between serum samples 3 and 5, whereas the (A)-rich regions varied among the three strains (Fig. 4B).

The secondary structure of 5′ UTR in strain JPN3/JAPAN/2013 was predicted according to the method described previously (8) (Fig. 4C). The stem-loops in the 5′ UTR were designated according to the stem-loops of the HCV 5′-UTR structures (30). Stem-loops (SLs) I, II, IIIa to IIIf, and the pseudoknot interaction were predicted within the 5′ UTR of strain JPN3/JAPAN/2013. These structures were the same as that of the strain reported previously (9), although several nucleotide insertions and deletions were more predominant in the apical loop of subdomain IIIb than in the other strains reported previously (Fig. 4A and C). Two seed sites of the microRNA miR-122 (Fig. 4A and C) were found in the 5′ UTR of strain JPN3/JAPAN/2013 at nucleotide residues 81 to 89 (UCCACAUUA) and 98 to 103 (CACUCC), which also corresponded to the predicted miR-122 seed sites in the 5′ UTRs of the other EHcV strains (9).

The HCV 3′ UTR, which is generally 200 to 300 nucleotides in length, consists of a short variable region, the poly(U/UC) stretch sequence, and the 3′-X-tail region, in that order (31–33). Although the EHcV 3′ UTR, which is composed of 138 nucleotides, is shorter than the HCV 3′ UTR, the 3′ UTR of EHcV consists of the (A)-rich sequence and 3′-X-tail region, in that order. The (A)-rich sequence of EHcV may vary in length (Fig. 4B). We subsequently predicted the secondary structure of the EHcV 3′ UTR. Although the EHcV 3′ UTR, which is composed of 138 nucleotides, is shorter than the HCV 3′ UTR, the 3′ UTR includes three predicted SL structures (Fig. 4C). Based on the SL structures in the HCV 3′ X-tail, these SL structures in the EHcV 3′ UTR were designated 3′SL I, 3′SL II, and 3′SL III, in that order from the 3′ terminus (Fig. 4C). Interestingly, the (A)-rich sequence was partially incorporated into the 3′SL III, although the poly(U/UC) stretch sequence in the HCV 3′ UTR is separated from any 3′SL structures (31–33). Furthermore, the two SL structures in the 3′ side of the EHcV NS5B-coding region were predicted to correspond to 5BSL3.2 and 5BSL3.3 in the NS5B-coding region of HCV. HCV 5BSL3.2 was previously shown to interact with 3′SL II to form the kissing-loop interaction, which is required for HCV replication (33). The secondary structure prediction shown in Fig. 4C suggests that the kissing-loop interaction may be conserved between 5BSL3.2 and the 3′SL II of the EHcV genome through their complementary sequences. The long-range RNA-RNA interaction between the apical loop of subdomain IIId in HCV IRES and the bulge of 5BSL3.2 supports IRES-dependent translation and viral RNA replication (34–36). In the case of the EHcV genome, the complement sequences were detected in the apical loops of subdomain and the 5BSL3.2-like subdomain (Fig. 4C), suggesting that the long-range RNA-RNA interaction may reside in the EHcV genome. These results indicated that HCV-like RNA secondary structures may be conserved around both UTRs of the EHcV genome.

Cleavage of the EHcV core protein by SPP. The C-terminal transmembrane region of the HCV core protein was previously shown to be cleaved by SPP following the cleavage of the core-E1 junction by signal peptidase (11, 28, 37). The core protein is known to be released from the precursor polyprotein embedded in the endoplasmic reticulum (ER) membrane, and it then moves

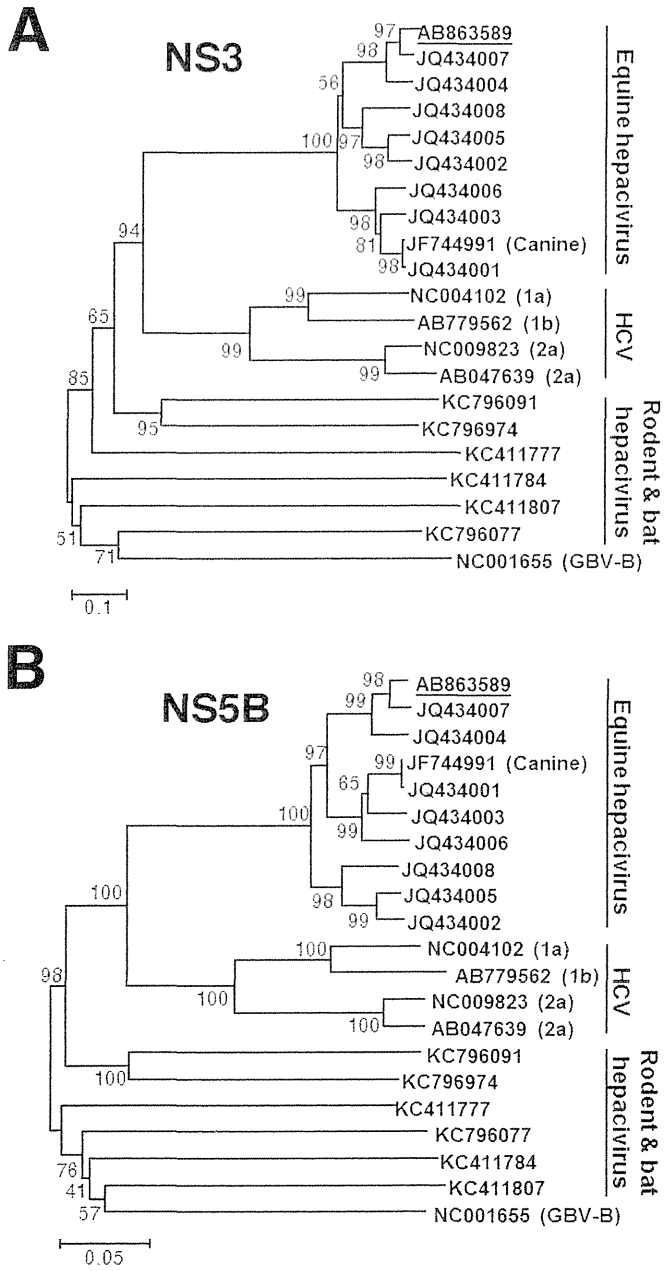

FIG 3 Phylogenetic analysis of the EHcV gene. Neighbor-joining trees of the nucleotide sequences from the NS3 (A) and NS5B (B) regions of the NPHV, HCV, and GBV-B strains are shown (23). Trees were constructed by the maximum composite likelihood method calculated using the program MEGA5 (24). The percentage of replicate trees in which the associated taxa were clustered together in the bootstrap test (1,000 replicates) is indicated next to the branches. Analyses were carried out using 10 strains of EhcV, JPN3/JAPAN/2013, A6-066 (GenBank accession no. JQ434003), B10-022 (GenBank accession no. JQ434004), F8-068 (GenBank accession no. JQ434005), G1-073 (GenBank accession no. JQ434002), G5-077 (GenBank accession no. JQ434006), H3-011 (GenBank accession no. JQ434008), H10-094 (GenBank accession no. JQ434007), NZP1 (GenBank accession no. JQ434001), and AAK-2011 (canine hepacivirus; GenBank accession no. JF744991); 4 strains of HCV, H77 (genotype 1a; GenBank accession no. NC004102), LyHCV (genotype 1b; GenBank accession no. AB779562), HC-J6CH (genotype 2a; GenBank accession no. NC009823), and JFH1 (genotype 2a; GenBank accession no. AB047639); 3 strains of bat hepacivirus, PDB-112 (GenBank accession no. KC796077), PDB-445 (GenBank accession no. KC796091), and PDB-829 (GenBank accession no. KC796074); 3 strains of rodent hepacivirus, RMU10-3382 (GenBank accession no. KC411777), NLR-AP-70 (GenBank accession no. KC411784), and SAR-46 (GenBank accession no. KC411807); and another primate hepacivirus, GBV-B (GenBank accession no. NC001655). The Japanese strain JPN3/JAPAN/2013 (GenBank accession no. AB863589) is underlined.

mainly to lipid droplets (LDs) (13, 14). Although SPP-dependent cleavage and LD translocation of the capsid protein are features common to HCV and GBV-B (13), it currently remains unknown whether the EHcV core protein shows these properties. The EHcV core protein shared 49.5% amino acid homology with the HCV core protein (genotype 1b) (Fig. 5A) and exhibited a hydrophobic/hydrophilic pattern similar to that of the HCV core protein (Fig. 5B). The EHcV core protein was predicted to be composed of domains 1, 2, and 3 relative to the HCV core protein. The transmembrane region of the EHcV core protein was predicted to span from Asn^{177} to Val^{199} by TMHMM2.0 (http://www.cbs.dtu.dk/services/TMHMM/). The transmembrane region of the EHcV core protein was 65% identical to that of the HCV core proteins (Fig. 5A). The C-terminal residue of the mature HCV core protein was found to be Phe^{177} in human and insect cell lines (17, 38). Our previous findings suggest that Ile^{176} and Phe^{177} of the HCV core protein may be responsible for SPP-dependent cleavage, because the replacement of Ile^{176} and Phe^{177} with Ala and Leu, respectively, abrogated intramembrane cleavage by SPP and impaired virus production (17, 28, 39). Weihofen et al. reported that SPP cleaved a peptide bond of the alpha-helix-breaking structure in a transmembrane region of the membrane protein (40). The replacement of Ile^{176} and Phe^{177} with Ala and Leu, respectively, in the HCV core protein converted the beta-sheet structure (alpha-helix-breaking structure) to an alpha-helix structure in the transmembrane region, as reported previously (28) (Fig. 6A and B). Ile^{190} and Phe^{191} of the EHcV core protein, which correspond to Ile^{176} and Phe^{177}, respectively, of the HCV core protein, reside in the alpha-helix-breaking structure of the transmembrane region (Fig. 6A and B). In contrast, the replacement of Ile^{190} and Phe^{191} with Ala and Leu, respectively, in the EHcV core protein were predicted to convert the beta-sheet to an alpha-helix structure in a manner similar to that for the HCV core protein (Fig. 6A and B). To investigate the involvement of SPP in the maturation of the EHcV core protein, we expressed EHcVc or HCVc in 293FT cells with an SPP or SPP mutant. These core proteins were expected to be resistant to signal peptidase-dependent processing because the C-terminal residue Ala of both core proteins was replaced with Arg, resulting in the detection of an immature core protein by the anti-HA antibody (Fig. 6A) (28). The core proteins with molecular masses of 23 kDa and 28 kDa were detected mainly with the anti-FLAG antibody in 293FT cells expressing HCVc and HCVc-mt, respectively (Fig. 6C, lanes 2 and 3); however, the 23-kDa band was not detected with the anti-HA antibody (Fig. 6C, lane 2). When EHcVc was expressed in 293FT cells, it was detected at a molecular mass of 27 kDa with the anti-FLAG antibody, but not with the anti-HA antibody (Fig. 6C, lane 4). In contrast, EHcV-mt, in which the 190th and 191st residues were Ala and Leu instead of Ile and Phe, respectively, was detected mainly at a molecular mass of 30 kDa with the anti-FLAG and anti-HA antibodies (Fig. 6C, lane 5). A loss-of-function SPP mutant (SPP-D219A) in which the 219th residue was Ala instead of Asp was shown to have a dominantly negative effect on SPP-dependent cleavage of the

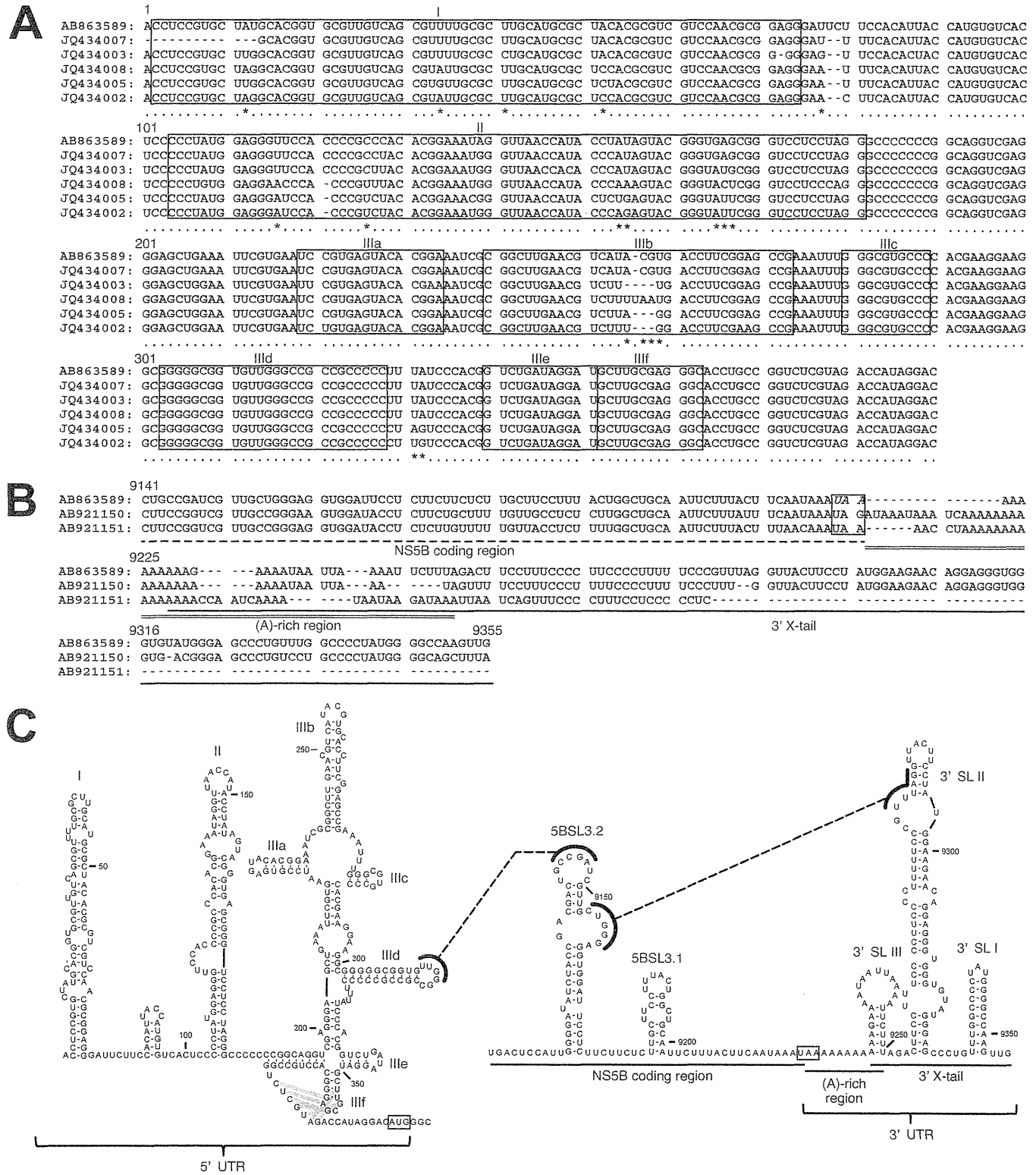

FIG 4 RNA structure analysis of the 5′ and 3′ ends of EHcV. (A) Alignment of the 5′ UTRs of the EHcV strains. Asterisks and black lines indicate variable residues and miRNA-targeting regions, respectively. SL structures are enclosed in rectangles. GenBank numbers are listed in the legend to Fig. 3. (B) Alignment of the 3′ UTRs of the EHcV strains. The 3′-terminal sequences with GenBank numbers AB921150 and AB921151 were determined using serum samples 5 and 1, respectively, and were aligned with that of JPN3/JAPAN/2013 (GenBank accession no. AB863589). (C) The secondary structures of the 5′ UTR, NS5B-coding region, and 3′ UTR were predicted on the basis of minimum free energy predictions. The stem loops in the 5′ UTR (left) were designated according to the stem loops of the HCV 5′-UTR structures (30). A gray line, double line, and single line indicate a pseudoknot structure, miR-122-target region, and complementary sequence, respectively. The stem loops in the NS5B-coding region and 3′ UTR (right) were designated to correspond to the stem loops embedded in the HCV 3′-terminal region (32, 33). The NS5B-coding region, (A)-rich region, and 3′-X-tail sequence are indicated under the schematic structure. Start and stop codons are enclosed by rectangles.

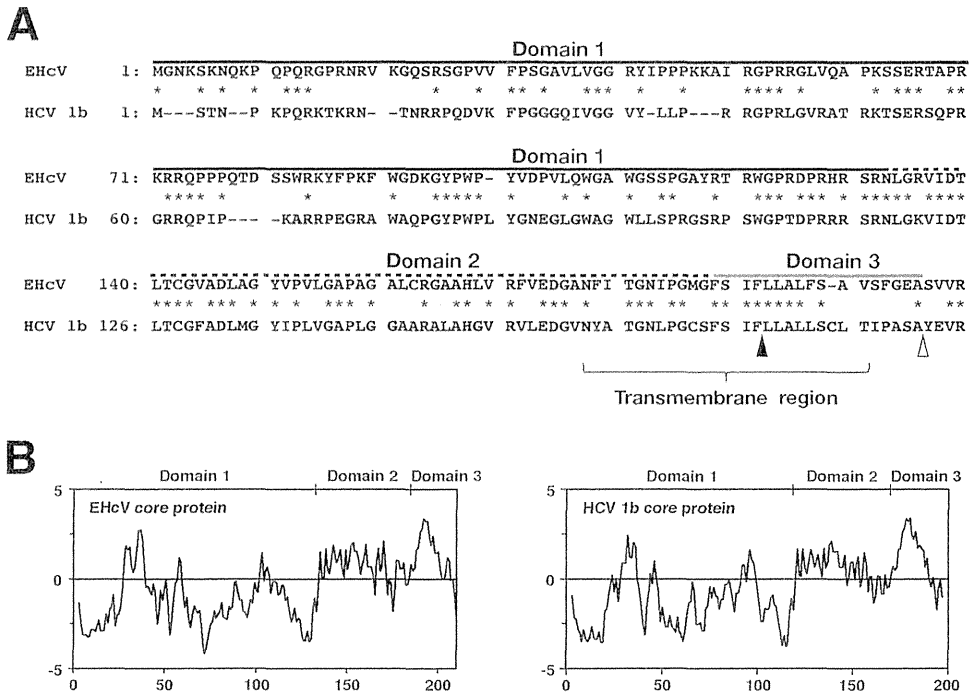

FIG 5 Amino acid alignment and hydrophobicity of EHcV and HCV core proteins. (A) Alignment of the core proteins of EHcV (JPN3/JAPAN/2013) and HCV genotype1b (Con1; GenBank accession number AJ238799). Asterisks indicate identical amino acid residues. Bars indicate gaps to achieve maximum amino acid matching. The black and white arrowheads indicate the predicted cleavage site of the core protein of HCV by SPP and signal peptidase, respectively. The EHcV core protein was composed of three domains, domain 1 (a black line, residues 2 to 132), domain 2 (a broken black line, residues 133 to 187), and domain 3 (a gray line, residues 188 to 204), relative to those of the HCV core protein (42). (B) Hydrophobicity plots of the EHcV and HCV core proteins were prepared by the method of Kyte and Doolittle (26). The horizontal and vertical axes represent amino acid position and hydrophobicity, respectively.

HCV core protein and to be coprecipitated with the immature core protein (28). HCVc had a molecular mass of 23 kDa in the presence of wild-type SPP (SPP-wt) and was detected with the anti-FLAG antibody, but not with the anti-HA antibody (Fig. 6D, lane 2), suggesting that the 23-kDa protein band may be a mature core protein. HCVc mainly had a molecular mass of 28 kDa in the presence of SPP-D219A and was detected with the anti-FLAG and anti-HA antibodies (Fig. 6D, lane 3), which corresponds to the mobility of HCVc-mt (Fig. 6D, lane 4). These results suggest that SPP-D219A may abrogate the intramembrane cleavage of HCVc. In a manner similar to that for the HCV core protein, EHcVc was detected mainly at a molecular mass of 27 kDa in the presence of SPP-wt with the anti-FLAG antibody, but not with the anti-HA antibody (Fig. 6D, lane 6). EHcVc was detected mainly at a molecular mass of 30 kDa in the presence of SPP-D219A with anti-FLAG and anti-HA antibodies (Fig. 6D, lane 7), corresponding to the mobility of EHcVc-mt (Fig. 6D, lane 8). When SPP-D219A was coexpressed with either HCVc or EHcVc, immature HCVc and EHcVc were coprecipitated with SPP-D219A (Fig. 6E, lanes 3 and 5). These results suggest that the EHcV core protein may be cleaved by SPP and that Ile^{190} and Phe^{191} of the EHcV core protein are critical for SPP-dependent cleavage.

The intracellular localization of the hepacivirus core protein. The HCV core protein is known to be localized mainly on the surface of LDs and is partially fractionated in the detergent-resistant membrane (DRM) close to the budding sites on the ER (13, 14, 16, 17). The core protein is considered to encompass the viral genome on the ER membrane, followed by budding into the lumen side (13, 14, 16, 17). To examine the intracellular localization of the EHcV core protein, we expressed HCVc or EHcVc in the Huh7OK1 cell line and stained the core proteins with the anti-FLAG antibody after staining LDs. Consistent with the findings of previous studies (14, 41, 42), HCVc was localized mainly on LDs (Fig. 7, row 3), whereas HCV-mt was not (Fig. 7, row 4). In a manner similar to that for the HCV core protein, EHcVc was localized mainly on LDs (Fig. 7, top row), whereas EHcVc-mt was not (Fig. 7, second row). These results suggest that the EHcV core protein may be localized mainly on LDs after SPP-dependent cleavage.

The DRM is defined as the cholesterol/sphingolipid-rich microdomain, which is resistant to nonionic detergents such as Triton X-100, considered to be a characteristic of lipid rafts. HCV was previously shown to be propagated in lipid raft-like compartments, including the membranous web (43–45). Furthermore, the HCV core protein is known to be associated with lipid raft-like compartments as well as LDs (16, 17, 41, 42). Therefore, we determined whether the EHcV core protein could be detected in the DRM fractions. EHcVc or EHcVc-mt was expressed in 293FT cells. The resulting cells were lysed on ice in the presence or absence of 1% Triton X-100. The DRM fractions were separated from the soluble proteins by a flotation assay with a stepwise density gradient in the presence or absence of Triton X-100. Serial fractions were collected after ultracentrifugation and were then subjected to Western blot analysis after being concentrated. EHcVc and EHcVc-mt were fractionated broadly from fractions of samples 3 to 11 without Triton X-100, and the fraction from

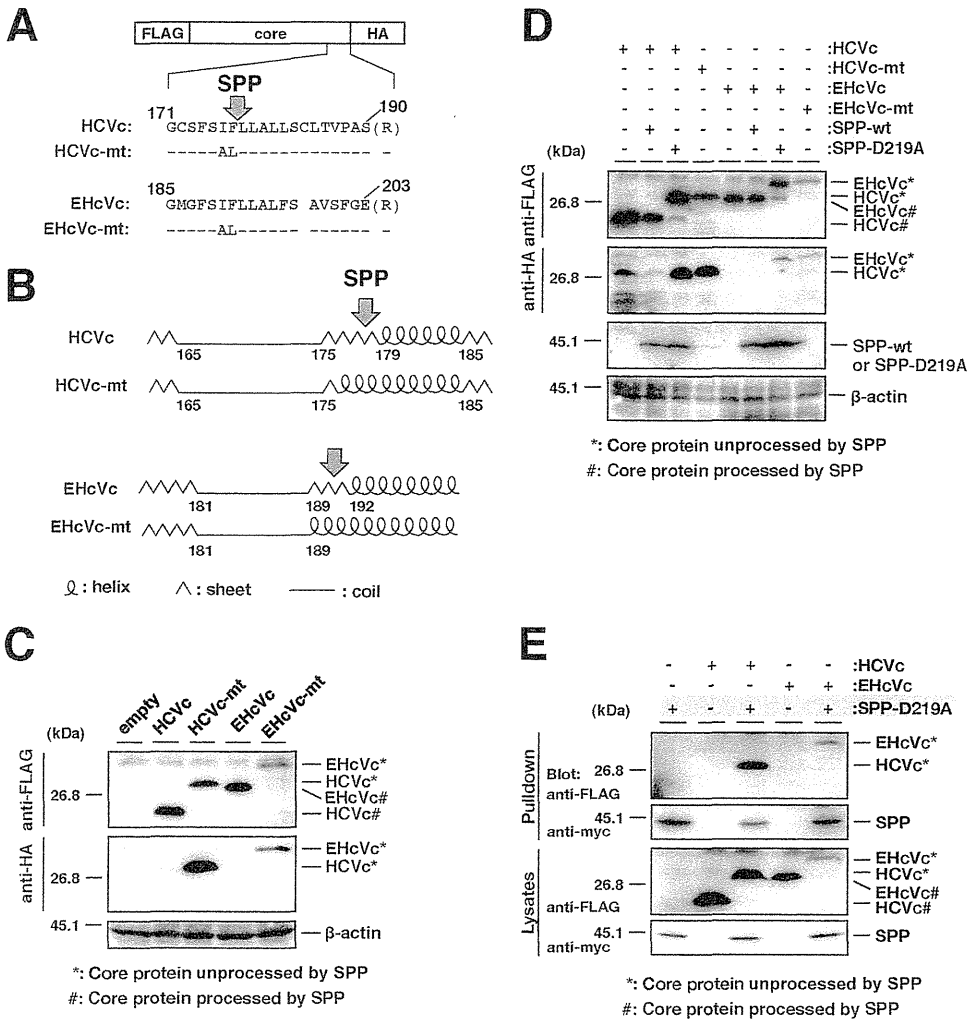

FIG 6 Intramembrane processing of the EHcV core protein by SPP. (A) The plasmids encoding HCVc, HCVc-mt, EHcVc, and EHcVc-mt are shown as a schematic diagram. Their C-terminal regions (171 to 190, HCV core protein; 185 to 203, EHcV core protein) were aligned. The C-terminal Ala of each core protein was replaced with Arg (R) to prevent signal peptidase-dependent cleavage for the detection of the SPP-uncleaved core protein with the anti-HA antibody. Bars indicate the amino acids that were the same as those of the wild-type residues. (B) The secondary protein structures in the C-terminal transmembrane regions of the HCV and EHcV core proteins and mutants were predicted by the method of Garnier et al. (25). Arrows indicate putative SPP cleavage sites. (C) HCVc, HCVc-mt, EHcVc, and EHcVc-mt were expressed in 293FT cells and immunoblotted with the anti-FLAG and -HA antibodies. (D) HCVc or EHcVc was expressed with SPP-wt or SPP-D219A in the 293FT cell line. HCVc-mt and EHcVc-mt were expressed in the absence of SPP-wt and SPP-D219A as uncleavable controls. (E) HCVc or EHcVc was coexpressed with or without SPP-D219A. SPP-D219A was pulled down with Ni beads. Coprecipitated proteins were immunoblotted with the anti-FLAG antibody.

sample 8 contained the largest amount of the core protein (Fig. 8, left panels). The distributions of the core proteins were roughly consistent with that of calreticulin, a marker protein of the ER membrane. When the cells expressing EHcVc were lysed in the presence of Triton X-100, a large amount of the core protein was localized in fractions 9 to 11 (Fig. 8, top three panels on the right). These fractions were enriched in calreticulin, corresponding to the detergent-soluble fractions (Fig. 8, fractions 7 to 11, top three panels on the right). However, EHcVc was partially detected in fractions 3 to 6 together with caveolin-1, a marker protein of the lipid raft (Fig. 8, fractions 3 to 6, top three panels on the right), suggesting that the EHcV core protein may have been partially distributed in the DRM fractions. In contrast, EHcVc-mt was localized in the detergent-soluble fractions (Fig. 8, fractions 9 to 11, bottom three panels on the right), but not in the DRM fractions (Fig. 8, fractions 3 to 6, bottom three panels on the right), in the presence of Triton X-100. EHcVc-mt was resistant to SPP-dependent processing, as described above (Fig. 6). These results suggest that the EHcV core protein may have been partially localized in the DRM and also that SPP-dependent processing may be required for DRM localization of the EHcV core protein.

DISCUSSION

The results of the present study indicate that EHcV infects Japanese-born domestic horses. Previous studies suggested that EHcV infected mainly horses and rarely dogs (5, 7–9). Our results demonstrate that EHcV commonly infects Japanese-born domestic horses (35.6% PCR positive and 22.6% seropositive). Several groups reported a prevalence of less than 10% PCR positivity in horses raised in the United States, the United Kingdom, and Ger-

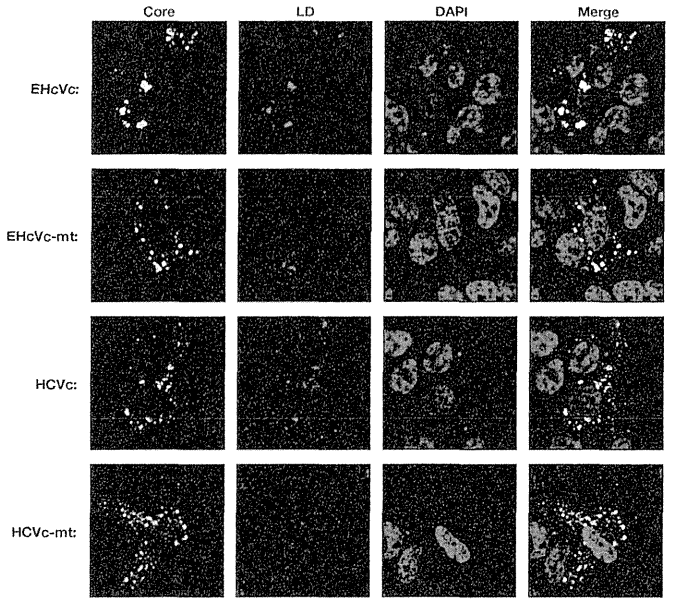

FIG 7 Intracellular localization of hepacivirus core proteins. HCVc, HCVc-mt, EHcVc, or EHcVc-mt was expressed in the Huh7OK1 cell line. The resulting cells were stained with Bodipy 558/568 (red) and then fixed with 4% paraformaldehyde at 24 h posttransfection, permeabilized, and subjected to indirect immunofluorescence staining. Each core protein was detected using mouse anti-FLAG antibodies and then Alexa 488-conjugated anti-mouse IgG (green). Cell nuclei were stained with DAPI after fixation (blue).

many (5, 7–9). Although the infection route of EHcV remains unknown, horses that were previously imported to Japan may be highly infected with EHcV. The serological prevalence in the present study appeared to be lower than that reported previously (8). A specific signal of the viral protein may be selected by Western blotting, used herein, rather than by the luciferase immunoprecipitation system, as reported previously (8), since the serum of each horse reacted to different proteins irrespective of the EHcV core protein (Fig. 2). The predicted full sequence of the EHcV strain amplified from serum sample 3 had high homology to those of the previously reported strains (Table 2). The polyproteins of previous strains had approximately 95% amino acid homology to one another irrespective of the area in which the horses originated, suggesting that these strains may belong to the same virological species. The parents of horse number 3 were born in Japan, while its grandparents were imported from the United States and Canada. Unfortunately, the sera of the parents and grandparents were not obtained in the present study. The EHcV strains obtained from Japanese-born horses may have originated from the United States or Canada. Another possibility is that one species of EHcV may have recently been distributed worldwide.

The primary and secondary structures of both UTRs are conserved among HCV strains and are essential for replication and translation. Four major stem-loop (SL) motifs have been detected in the 5′ UTR of the HCV genome, three SL structures of which are known to be required for IRES activity (46). Domain IIId plays a crucial role in anchoring of the 40S ribosome for IRES activity (47). Domain IIIb and the four-way helical junction of domains IIIa, IIIb, and IIIc bind eukaryotic initiation factor 3 (eIF3) and form a ternary complex, thereby forming the 48S preinitiation complex on HCV RNA (48). Moreover, domain II is known to be required to enhance eIF5-mediated GTP hydrolysis and the release of eIF2 from the 48S complex (48). These equivalent motifs were observed in the predicted secondary structures of the 5′ UTR of the reported EHcV strains (49), as well as in strain JPN3/JAPAN/2013 in the present study (Fig. 4C). A recent study demonstrated that the EHcV 5′ UTR exhibited IRES-dependent translation activity (50); however, further studies are needed to fully understand the IRES activity of the EHcV 5′UTR.

SL motifs embedded in the NS5B-coding region and UTRs of the HCV genome are known to be associated with viral replication. Several studies found that the mutational disruption of the complement sequence between 5BSL3.2 and 3′SL2 inhibited HCV RNA replication (33, 51). Additionally, the apical loop of domain IIId in the HCV 5′ UTR was shown to interact with the bulge of 5BSL3.2, supporting IRES-dependent translation and viral RNA replication (34–36). The RNA secondary structures of the 3′ UTR in the EHcV genome remained unknown due to limited information on its nucleotide sequence. 3′ RACE using poly(U) polymerase was employed in the present study because the ordinary 3′-RACE reaction using poly(A) polymerase was stopped at the (A)-rich region of the EHcV 3′ UTR. The nucleotide sequence of the EHcV 3′ UTR was determined, and its RNA secondary structure was then predicted (Fig. 4B and C). The results of the present

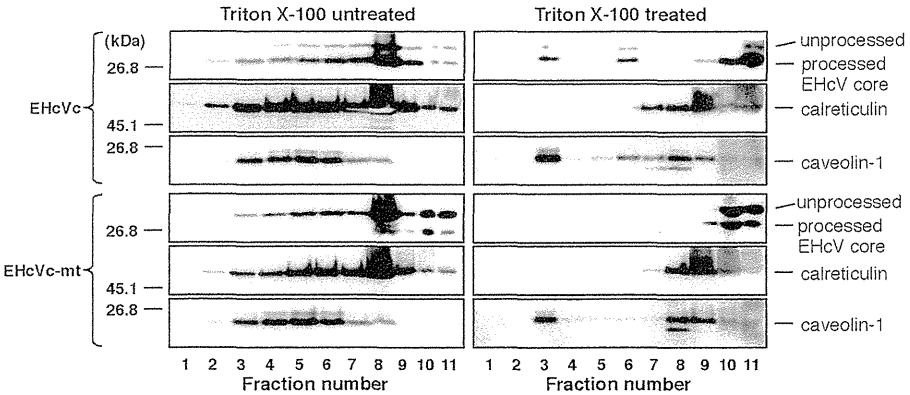

FIG 8 The EHcV core protein partially migrated to the DRM fraction after SPP-dependent processing. 293FT cells expressing either EHcVc or EHcVc-mt were homogenized with or without 1% Triton X-100 and then subjected to a flotation assay. Proteins in each fraction were concentrated with cold acetone and then subjected to Western blotting using the anti-FLAG, anti-calreticulin, or anti-caveolin-1 antibody.

study revealed that the 3′ UTR of the EHcV genome consists of the (A)-rich sequence and relatively shorter 3′-X-tail sequence. The three SL structures of the EHcV 3′ UTR were similar to those of the HCV 3′ UTR but were markedly different from the 3′ UTRs of GBV-B and rodent hepaciviruses. Drexler et al. described the structural characteristics of the 5′ and 3′ UTRs in rodent hepacivirus as well as phylogenetic information, liver tropism, and the pathogenicity of the virus (5). The SL motifs embedded in the 3′ X-tails of rodent hepacivirus and GBV-B varied. The structures of the 3′ UTRs appeared to correspond to the phylogenetic relationship of the hepaciviruses (5). Figure 4C shows that there were two stem-loop structures within the NS5B-coding region of EHcV corresponding to 5BSL3.2 and 5BSL3.3 of HCV RNA. Complementary regions were observed between the 5BSL3.2-like domain and 3′SL2, as well as between the 5BSL3.2-like domain and domain IIId of the EHcV genome (Fig. 4B and C). The kissing-loop and long-range RNA-RNA interactions may be structurally conserved between EHcV and HCV. Functional analyses of the *cis*-acting elements of the EHcV genome will contribute to the establishment of an EHcV infection system.

The mature HCV core protein was previously shown to be generated from the viral precursor polyprotein by signal peptidase followed by SPP-dependent processing of the transmembrane region (52). The core proteins of HCV and GBV-B are known to be cleaved by SPP (12, 37). The transmembrane regions of both the HCV and EHcV core proteins were found to be structurally conserved, based on their amino acid sequences and hydrophobicity plots (Fig. 5A and B and Fig. 6B). The replacement of Ile^{190} and Phe^{191} with Ala and Leu, respectively, in the EHcV core protein abrogated the intramembrane processing of the EHcV core protein (Fig. 6C). The loss-of-function mutant of SPP inhibited intramembrane processing of the EHcV core protein (Fig. 6D). Furthermore, the loss-of-function mutant of SPP specifically interacted with an uncleaved form of the EHcV core protein (Fig. 6E). These results indicate that the transmembrane region of the EHcV core protein may have been cleaved by SPP. The mature HCV core protein is known to be translocated into LDs and partially on lipid raft-like membranes. Previous studies reported that the HCV core protein on the LDs may be recruited near the replication complex in the membranous web, which consists of cholesterol- and sphingolipid-rich lipid components (43–45). Viral assembly was shown to occur on the ER membrane close to LDs and the membranous web (14). In addition to the HCV core protein, the nonstructural proteins and viral RNA of HCV were detected in the DRM fractions. The HCV RNA polymerase NS5B was previously reported to interact with sphingomyelin (53). Furthermore, a serine palmitoyltransferase inhibitor suppressed HCV replication by disrupting the replication complex (53, 54). These findings indicate that the DRM is provided as a scaffold for the formation of the HCV replication complex (45, 54). In the present study, we showed that the mature EHcV core protein was localized mainly on LDs and partially on the DRM (Fig. 7 and 8). A mutational analysis of the EHcV core protein indicated that SPP-dependent cleavage may be required for the localization of the EHcV core protein on LDs and the DRM in a manner similar to that for the HCV core protein. In addition, the assembly mechanism of EHcV may be similar to that of HCV.

In conclusion, the results of the present study show that EHcV shares common features with the HCV genomic structure and the biological properties of the capsid protein. *In vivo* and *ex vivo* infection systems for EHcV have not yet been successfully established. SCID mice carrying chimeric human livers are currently employed as a small animal model for *in vivo* infection with HCV (55) but are not suitable for studies on immunity and pathogenicity due to an immunodeficiency. Chimpanzees are not yet available for *in vivo* HCV research. Further studies on the mechanisms underlying EHcV infection will contribute to the development of an *in vivo* surrogate model system for studying HCV immunity and pathogenicity.

ACKNOWLEDGMENTS

We thank M. Furugori for her secretarial work, I. Katoh for helpful discussions, and C. Endoh for technical assistance.

This work was supported by Grants-in-Aid from the Ministry of Health, Labor, and Welfare, Japan (H24-Kanen-008 and H25-Kanen-002 and -008); the Ministry of Education, Culture, Sports, Science, and Technology, Japan; and the Japan Science and Technology Agency (JST) (Houga-24659204).

REFERENCES

1. **Simons JN, Leary TP, Dawson GJ, Pilot-Matias TJ, Muerhoff AS, Schlauder GG, Desai SM, Mushahwar IK.** 1995. Isolation of novel virus-like sequences associated with human hepatitis. Nat. Med. **1**:564–569. http://dx.doi.org/10.1038/nm0695-564.
2. **Beames B, Chavez D, Lanford RE.** 2001. GB virus B as a model for hepatitis C virus. ILAR J. **42**:152–160. http://dx.doi.org/10.1093/ilar.42.2.152.
3. **Bukh J, Apgar CL, Govindarajan S, Purcell RH.** 2001. Host range studies of GB virus-B hepatitis agent, the closest relative of hepatitis C virus, in New World monkeys and chimpanzees. J. Med. Virol. **65**:694–697. http://dx.doi.org/10.1002/jmv.2092.
4. **Quan PL, Firth C, Conte JM, Williams SH, Zambrana-Torrelio CM, Anthony SJ, Ellison JA, Gilbert AT, Kuzmin IV, Niezgoda M, Osinubi MO, Recuenco S, Markotter W, Breiman RF, Kalemba L, Malekani J, Lindblade KA, Rostal MK, Ojeda-Flores R, Suzan G, Davis LB, Blau DM, Ogunkoya AB, Alvarez Castillo DA, Moran D, Ngam S, Akaibe D, Agwanda B, Briese T, Epstein JH, Daszak P, Rupprecht CE, Holmes EC, Lipkin WI.** 2013. Bats are a major natural reservoir for hepaciviruses and pegiviruses. Proc. Natl. Acad. Sci. U. S. A. **110**:8194–8199. http://dx.doi.org/10.1073/pnas.1303037110.
5. **Drexler JF, Corman VM, Muller MA, Lukashev AN, Gmyl A, Coutard B, Adam A, Ritz D, Leijten LM, van Riel D, Kallies R, Klose SM, Gloza-Rausch F, Binger T, Annan A, Adu-Sarkodie Y, Oppong S, Bourgarel M, Rupp D, Hoffmann B, Schlegel M, Kummerer BM, Kruger DH, Schmidt-Chanasit J, Setien AA, Cottontail VM, Hemachudha T, Wacharapluesadee S, Osterrieder K, Bartenschlager R, Matthee S, Beer M, Kuiken T, Reusken C, Leroy EM, Ulrich RG, Drosten C.** 2013. Evidence for novel hepaciviruses in rodents. PLoS Pathog. **9**:e1003438. http://dx.doi.org/10.1371/journal.ppat.1003438.
6. **Kapoor A, Simmonds P, Scheel TK, Hjelle B, Cullen JM, Burbelo PD, Chauhan LV, Duraisamy R, Sanchez Leon M, Jain K, Vandegrift KJ, Calisher CH, Rice CM, Lipkin WI.** 2013. Identification of rodent homologs of hepatitis C virus and pegiviruses. mBio **4**(2):e00216–13. http://dx.doi.org/10.1128/mBio.00216-13.
7. **Lyons S, Kapoor A, Sharp C, Schneider BS, Wolfe ND, Culshaw G, Corcoran B, McGorum BC, Simmonds P.** 2012. Nonprimate hepaciviruses in domestic horses, United Kingdom. Emerg. Infect. Dis. **18**:1976–1982. http://dx.doi.org/10.3201/eid1812.120498.
8. **Burbelo PD, Dubovi EJ, Simmonds P, Medina JL, Henriquez JA, Mishra N, Wagner J, Tokarz R, Cullen JM, Iadarola MJ, Rice CM, Lipkin WI, Kapoor A.** 2012. Serology-enabled discovery of genetically diverse hepaciviruses in a new host. J. Virol. **86**:6171–6178. http://dx.doi.org/10.1128/JVI.00250-12.
9. **Kapoor A, Simmonds P, Gerold G, Qaisar N, Jain K, Henriquez JA, Firth C, Hirschberg DL, Rice CM, Shields S, Lipkin WI.** 2011. Characterization of a canine homolog of hepatitis C virus. Proc. Natl. Acad. Sci. U. S. A. **108**:11608–11613. http://dx.doi.org/10.1073/pnas.1101794108.
10. **van der Laan LJ, de Ruiter PE, van Gils IM, Fieten H, Spee B, Pan Q, Rothuizen J, Penning LC.** 5 June 2014. Canine hepacivirus and idiopathic

hepatitis in dogs from a Dutch cohort. J. Viral Hepat. http://dx.doi.org/10.1111/jvh.12268.
11. Hüssy P, Langen H, Mous J, Jacobsen H. 1996. Hepatitis C virus core protein: carboxy-terminal boundaries of two processed species suggest cleavage by a signal peptide peptidase. Virology 224:93–104. http://dx.doi.org/10.1006/viro.1996.0510.
12. Targett-Adams P, Schaller T, Hope G, Lanford RE, Lemon SM, Martin A, McLauchlan J. 2006. Signal peptide peptidase cleavage of GB virus B core protein is required for productive infection in vivo. J. Biol. Chem. 281:29221–29227. http://dx.doi.org/10.1074/jbc.M605373200.
13. Hope RG, Murphy DJ, McLauchlan J. 2002. The domains required to direct core proteins of hepatitis C virus and GB virus-B to lipid droplets share common features with plant oleosin proteins. J. Biol. Chem. 277:4261–4270. http://dx.doi.org/10.1074/jbc.M108798200.
14. Miyanari Y, Atsuzawa K, Usuda N, Watashi K, Hishiki T, Zayas M, Bartenschlager R, Wakita T, Hijikata M, Shimotohno K. 2007. The lipid droplet is an important organelle for hepatitis C virus production. Nat. Cell Biol. 9:1089–1097. http://dx.doi.org/10.1038/ncb1631.
15. Samsa MM, Mondotte JA, Iglesias NG, Assuncao-Miranda I, Barbosa-Lima G, Da Poian AT, Bozza PT, Gamarnik AV. 2009. Dengue virus capsid protein usurps lipid droplets for viral particle formation. PLoS Pathog. 5:e1000632. http://dx.doi.org/10.1371/journal.ppat.1000632.
16. Matto M, Rice CM, Aroeti B, Glenn JS. 2004. Hepatitis C virus core protein associates with detergent-resistant membranes distinct from classical plasma membrane rafts. J. Virol. 78:12047–12053. http://dx.doi.org/10.1128/JVI.78.21.12047-12053.2004.
17. Okamoto K, Mori Y, Komoda Y, Okamoto T, Okochi M, Takeda M, Suzuki T, Moriishi K, Matsuura Y. 2008. Intramembrane processing by signal peptide peptidase regulates the membrane localization of hepatitis C virus core protein and viral propagation. J. Virol. 82:8349–8361. http://dx.doi.org/10.1128/JVI.00306-08.
18. Aizaki H, Lee KJ, Sung VM, Ishiko H, Lai MM. 2004. Characterization of the hepatitis C virus RNA replication complex associated with lipid rafts. Virology 324:450–461. http://dx.doi.org/10.1016/j.virol.2004.03.034.
19. Egger D, Wolk B, Gosert R, Bianchi L, Blum HE, Moradpour D, Bienz K. 2002. Expression of hepatitis C virus proteins induces distinct membrane alterations including a candidate viral replication complex. J. Virol. 76:5974–5984. http://dx.doi.org/10.1128/JVI.76.12.5974-5984.2002.
20. Marchuk D, Drumm M, Saulino A, Collins FS. 1991. Construction of T-vectors, a rapid and general system for direct cloning of unmodified PCR products. Nucleic Acids Res. 19:1154. http://dx.doi.org/10.1093/nar/19.5.1154.
21. Tajima S, Takasaki T, Matsuno S, Nakayama M, Kurane I. 2005. Genetic characterization of Yokose virus, a flavivirus isolated from the bat in Japan. Virology 332:38–44. http://dx.doi.org/10.1016/j.virol.2004.06.052.
22. Tilgner M, Shi PY. 2004. Structure and function of the 3′ terminal six nucleotides of the West Nile virus genome in viral replication. J. Virol. 78:8159–8171. http://dx.doi.org/10.1128/JVI.78.15.8159-8171.2004.
23. Saitou N, Nei M. 1987. The neighbor-joining method: a new method for reconstructing phylogenetic trees. Mol. Biol. Evol. 4:406–425.
24. Tamura K, Peterson D, Peterson N, Stecher G, Nei M, Kumar S. 2011. MEGA5: molecular evolutionary genetics analysis using maximum likelihood, evolutionary distance, and maximum parsimony methods. Mol. Biol. Evol. 28:2731–2739. http://dx.doi.org/10.1093/molbev/msr121.
25. Garnier J, Osguthorpe DJ, Robson B. 1978. Analysis of the accuracy and implications of simple methods for predicting the secondary structure of globular proteins. J. Mol. Biol. 120:97–120. http://dx.doi.org/10.1016/0022-2836(78)90297-8.
26. Kyte J, Doolittle RF. 1982. A simple method for displaying the hydropathic character of a protein. J. Mol. Biol. 157:105–132. http://dx.doi.org/10.1016/0022-2836(82)90515-0.
27. Zuker M. 2003. Mfold web server for nucleic acid folding and hybridization prediction. Nucleic Acids Res. 31:3406–3415. http://dx.doi.org/10.1093/nar/gkg595.
28. Okamoto K, Moriishi K, Miyamura T, Matsuura Y. 2004. Intramembrane proteolysis and endoplasmic reticulum retention of hepatitis C virus core protein. J. Virol. 78:6370–6380. http://dx.doi.org/10.1128/JVI.78.12.6370-6380.2004.
29. Okamoto T, Nishimura Y, Ichimura T, Suzuki K, Miyamura T, Suzuki T, Moriishi K, Matsuura Y. 2006. Hepatitis C virus RNA replication is regulated by FKBP8 and Hsp90. EMBO J. 25:5015–5025. http://dx.doi.org/10.1038/sj.emboj.7601367.
30. Honda M, Brown EA, Lemon SM. 1996. Stability of a stem-loop involving the initiator AUG controls the efficiency of internal initiation of translation on hepatitis C virus RNA. RNA 2:955–968.
31. Yanagi M, St Claire M, Emerson SU, Purcell RH, Bukh J. 1999. In vivo analysis of the 3′ untranslated region of the hepatitis C virus after in vitro mutagenesis of an infectious cDNA clone. Proc. Natl. Acad. Sci. U. S. A. 96:2291–2295. http://dx.doi.org/10.1073/pnas.96.5.2291.
32. Blight KJ, Rice CM. 1997. Secondary structure determination of the conserved 98-base sequence at the 3′ terminus of hepatitis C virus genome RNA. J. Virol. 71:7345–7352.
33. Friebe P, Boudet J, Simorre JP, Bartenschlager R. 2005. Kissing-loop interaction in the 3′ end of the hepatitis C virus genome essential for RNA replication. J. Virol. 79:380–392. http://dx.doi.org/10.1128/JVI.79.1.380-392.2005.
34. Lourenço S, Costa F, Debarges B, Andrieu T, Cahour A. 2008. Hepatitis C virus internal ribosome entry site-mediated translation is stimulated by cis-acting RNA elements and trans-acting viral factors. FEBS J. 275:4179–4197. http://dx.doi.org/10.1111/j.1742-4658.2008.06566.x.
35. Cristina J, del Pilar Moreno M, Moratorio G. 2007. Hepatitis C virus genetic variability in patients undergoing antiviral therapy. Virus Res. 127:185–194. http://dx.doi.org/10.1016/j.virusres.2007.02.023.
36. Song Y, Friebe P, Tzima E, Junemann C, Bartenschlager R, Niepmann M. 2006. The hepatitis C virus RNA 3′-untranslated region strongly enhances translation directed by the internal ribosome entry site. J. Virol. 80:11579–11588. http://dx.doi.org/10.1128/JVI.00675-06.
37. McLauchlan J, Lemberg MK, Hope G, Martoglio B. 2002. Intramembrane proteolysis promotes trafficking of hepatitis C virus core protein to lipid droplets. EMBO J. 21:3980–3988. http://dx.doi.org/10.1093/emboj/cdf414.
38. Ogino T, Fukuda H, Imajoh-Ohmi S, Kohara M, Nomoto A. 2004. Membrane binding properties and terminal residues of the mature hepatitis C virus capsid protein in insect cells. J. Virol. 78:11766–11777. http://dx.doi.org/10.1128/JVI.78.21.11766-11777.2004.
39. Kopp M, Murray CL, Jones CT, Rice CM. 2010. Genetic analysis of the carboxy-terminal region of the hepatitis C virus core protein. J. Virol. 84:1666–1673. http://dx.doi.org/10.1128/JVI.02043-09.
40. Weihofen A, Binns K, Lemberg MK, Ashman K, Martoglio B. 2002. Identification of signal peptide peptidase, a presenilin-type aspartic protease. Science 296:2215–2218. http://dx.doi.org/10.1126/science.1070925.
41. Barba G, Harper F, Harada T, Kohara M, Goulinet S, Matsuura Y, Eder G, Schaff Z, Chapman MJ, Miyamura T, Brechot C. 1997. Hepatitis C virus core protein shows a cytoplasmic localization and associates to cellular lipid storage droplets. Proc. Natl. Acad. Sci. U. S. A. 94:1200–1205. http://dx.doi.org/10.1073/pnas.94.4.1200.
42. Hope RG, McLauchlan J. 2000. Sequence motifs required for lipid droplet association and protein stability are unique to the hepatitis C virus core protein. J. Gen. Virol. 81:1913–1925.
43. Gao L, Aizaki H, He JW, Lai MM. 2004. Interactions between viral nonstructural proteins and host protein hVAP-33 mediate the formation of hepatitis C virus RNA replication complex on lipid raft. J. Virol. 78:3480–3488. http://dx.doi.org/10.1128/JVI.78.7.3480-3488.2004.
44. Gosert R, Egger D, Lohmann V, Bartenschlager R, Blum HE, Bienz K, Moradpour D. 2003. Identification of the hepatitis C virus RNA replication complex in Huh-7 cells harboring subgenomic replicons. J. Virol. 77:5487–5492. http://dx.doi.org/10.1128/JVI.77.9.5487-5492.2003.
45. Shi ST, Lee KJ, Aizaki H, Hwang SB, Lai MM. 2003. Hepatitis C virus RNA replication occurs on a detergent-resistant membrane that cofractionates with caveolin-2. J. Virol. 77:4160–4168. http://dx.doi.org/10.1128/JVI.77.7.4160-4168.2003.
46. Tsukiyama-Kohara K, Iizuka N, Kohara M, Nomoto A. 1992. Internal ribosome entry site within hepatitis C virus RNA. J. Virol. 66:1476–1483.
47. Babaylova E, Graifer D, Malygin A, Stahl J, Shatsky I, Karpova G. 2009. Positioning of subdomain IIId and apical loop of domain II of the hepatitis C IRES on the human 40S ribosome. Nucleic Acids Res. 37:1141–1151. http://dx.doi.org/10.1093/nar/gkn1026.
48. Kieft JS, Zhou K, Grech A, Jubin R, Doudna JA. 2002. Crystal structure of an RNA tertiary domain essential to HCV IRES-mediated translation initiation. Nat. Struct. Biol. 9:370–374. http://dx.doi.org/10.1038/nsb781.
49. Locker N, Easton LE, Lukavsky PJ. 2007. HCV and CSFV IRES domain II mediate eIF2 release during 80S ribosome assembly. EMBO J. 26:795–805. http://dx.doi.org/10.1038/sj.emboj.7601549.

50. Stewart H, Walter C, Jones D, Lyons S, Simmonds P, Harris M. 2013. The non-primate hepacivirus 5′ untranslated region possesses internal ribosomal entry site activity. J. Gen. Virol. 94:2657–2663. http://dx.doi.org/10.1099/vir.0.055764-0.
51. Diviney S, Tuplin A, Struthers M, Armstrong V, Elliott RM, Simmonds P, Evans DJ. 2008. A hepatitis C virus *cis*-acting replication element forms a long-range RNA-RNA interaction with upstream RNA sequences in NS5B. J. Virol. 82:9008–9022. http://dx.doi.org/10.1128/JVI.02326-07.
52. Penin F, Dubuisson J, Rey FA, Moradpour D, Pawlotsky JM. 2004. Structural biology of hepatitis C virus. Hepatology 39:5–19. http://dx.doi.org/10.1002/hep.20032.
53. Hirata Y, Ikeda K, Sudoh M, Tokunaga Y, Suzuki A, Weng L, Ohta M, Tobita Y, Okano K, Ozeki K, Kawasaki K, Tsukuda T, Katsume A, Aoki Y, Umehara T, Sekiguchi S, Toyoda T, Shimotohno K, Soga T, Nishijima M, Taguchi R, Kohara M. 2012. Self-enhancement of hepatitis C virus replication by promotion of specific sphingolipid biosynthesis. PLoS Pathog. 8:e1002860. http://dx.doi.org/10.1371/journal.ppat.1002860.
54. Katsume A, Tokunaga Y, Hirata Y, Munakata T, Saito M, Hayashi H, Okamoto K, Ohmori Y, Kusanagi I, Fujiwara S, Tsukuda T, Aoki Y, Klumpp K, Tsukiyama-Kohara K, El-Gohary A, Sudoh M, Kohara M. 2013. A serine palmitoyltransferase inhibitor blocks hepatitis C virus replication in human hepatocytes. Gastroenterology 145:865–873. http://dx.doi.org/10.1053/j.gastro.2013.06.012.
55. Mercer DF, Schiller DE, Elliott JF, Douglas DN, Hao C, Rinfret A, Addison WR, Fischer KP, Churchill TA, Lakey JR, Tyrrell DL, Kneteman NM. 2001. Hepatitis C virus replication in mice with chimeric human livers. Nat. Med. 7:927–933. http://dx.doi.org/10.1038/90968.

Hepatology Research

Hepatology Research 2014 doi: 10.1111/hepr.12377

Original Article

Liver stiffness measurement for risk assessment of hepatocellular carcinoma

Akihisa Tatsumi,[1] Shinya Maekawa,[1] Mitsuaki Sato,[1] Nobutoshi Komatsu,[1] Mika Miura,[1] Fumitake Amemiya,[2] Yasuhiro Nakayama,[1] Taisuke Inoue,[1] Minoru Sakamoto[1] and Nobuyuki Enomoto[1]

[1]*First Department of Medicine, University of Yamanashi, Chuo, and* [2]*Department of Gastroenterological Medicine, Kofu Municipal Hospital, Kofu, Yamanashi, Japan*

Aim: Liver fibrosis is a risk factor for hepatocellular carcinoma (HCC), but at what fibrotic stage the risk for HCC is increased has been poorly investigated quantitatively. This study aimed to determine the appropriate cut-off value of liver stiffness for HCC concurrence by FibroScan, and its clinical significance in hepatitis B virus (HBV), hepatitis C virus (HCV) and non-B, non-C (NBNC) liver disease.

Methods: Subjects comprised 1002 cases (246 with HCC and 756 without HCC) with chronic liver disease (HBV, 104; HCV, 722; and NBNC, 176).

Results: Liver stiffness was significantly greater in all groups with HCC, and the determined cut-off value for HCC concurrence was more than 12.0 kPa in those with HCV, more than 8.5 kPa in those with HBV and more than 12.0 kPa in those with NBNC. Liver stiffness of more than 12.0 kPa was an independent risk factor for new HCC development in HCV. For HCV, risk factors for HCC concurrence were old age, male sex, low albumin, low platelets and liver stiffness, while for HBV they were old age, low platelets and liver stiffness, and for NBNC they were old age, elevated α-fetoprotein and liver stiffness.

Conclusion: Liver stiffness cut-off values and their association with HCC concurrence were different depending on the etiology. In HCV, liver stiffness of more than 12.0 kPa was an independent risk factor for new HCC development. Collectively, determining the fibrotic cut-off values for HCC concurrence would be important in evaluating HCC risks.

Key words: FibroScan, hepatocellular carcinoma, liver fibrosis

INTRODUCTION

HEPATOCELLULAR CARCINOMA (HCC) is the fifth most common cancer in the world and the third most common cause of cancer deaths.[1] HCC, accounting for 90% of primary liver cancer, is a global clinical issue.[2] For improvement in the prognosis of HCC, curative therapy following early detection is important. To this end, it is critical to identify high-risk groups for HCC and perform appropriate surveillance in the clinical practice of chronic liver disease. It has been postulated that hepatitis virus infection, old age, male sex, alanine aminotransferase (ALT) elevation, liver fibrosis, and low albumin (Alb), low platelets (Plt) and α-fetoprotein (AFP) elevation are risk factors for HCC; however, liver fibrosis is the most important risk factor irrespective of its etiology.[3–6]

To date, liver fibrosis has been evaluated by liver biopsy, but it is associated with several problems such as invasiveness, sampling errors, semiquantitation and diagnostic differences among pathologists. With the development of FibroScan (Echosens, Paris, France) using transient elastography, it has become possible to quantitate liver elasticity non-invasively.[7] The diagnostic accuracy of FibroScan for liver fibrosis has been recognized widely for various chronic liver diseases with the exception of some liver conditions such as congestion,

Correspondence: Dr Nobuyuki Enomoto, First Department of Medicine, University of Yamanashi, 1110 Shimokato, Chuo, Yamanashi 409-3898, Japan. Email: enomoto@yamanashi.ac.jp

Financial disclosure: This study was supported in part by Grants-in-Aid from the Ministry of Education, Science, Sports and Culture of Japan (23390195, 23791404, 24590964 and 24590965), and in part by Grants-in-Aid from the Ministry of Health, Labour and Welfare of Japan (H23-kanen-001, H23-kanen-004, H23-kanen-006, H24-kanen-002, H24-kanen-004 and H25-kanen-006).

Received 27 December 2013; revision 22 May 2014; accepted 14 June 2014.

severe inflammation or cholestasis in which liver fibrosis might be overestimated with FibroScan.[8–12] The risk for HCC is evaluable based on liver stiffness measured by FibroScan in cases with hepatitis B virus (HBV) and hepatitis C virus (HCV).[12–19] Nevertheless, in most reports the risk for HCC was only indirectly evaluated based on the value for liver cirrhosis as measured by FibroScan. Liver stiffness related to HCC has not been directly evaluated. Furthermore, the utility of FibroScan in evaluation of the risk for HCC has not been elucidated in non-B, non-C (NBNC) liver disease.

In this study, liver stiffness in patients with chronic liver disease was quantitatively measured and liver stiffness related to HCC occurrence was elucidated separately in cases with HCV, HBV and NBNC liver disease for investigations of its clinical utility.

METHODS

Patients

THE SUBJECTS COMPRISED 1002 patients with chronic liver disease whose liver stiffness was measured by FibroScan consecutively at the University of Yamanashi Hospital between January 2010 and December 2012. Informed consent had been obtained for measurement of liver stiffness before the modality was approved by the national insurance in October 2011. The HCV group (722 cases including 66 sustained virological response [SVR] cases), HBV group (104 cases) and NBNC group (176 cases) were defined as HCV antibody positive, hepatitis B surface antigen (HBsAg) positive, and HBsAg negative and HCV antibody negative cases, respectively. Both HBsAg and HCV antibody positive cases ($n = 3$) and HIV co-infection cases (co-infection with HBV, $n = 1$) were excluded. HCC cases included those with a history of HCC. Among the 1002 cases with chronic liver disease, 246 had HCC and 756 were without HCC. Of those without HCC, 470 hepatitis C cases were followed up by abdominal ultrasonography, contrast computed tomography (CT) or ethoxybenzyl (EOB) contrast magnetic resonance imaging (MRI) every 3–6 months. HCC was diagnosed by contrast ultrasonography, contrast enhancement in the arterial phase and poor enhancement at the equilibrium phase in contrast CT (including CT arteriography and computed tomographic arterial portography) and contrast MRI, and histology by liver tumor biopsy. According to the Declaration of Helsinki, this study was performed after approval was obtained by the ethical committee of the Faculty of Medicine, University of Yamanashi.

Measurement of liver stiffness

FibroScan502 (Echosens) was used for measurement with the M-probe and L-probe. Patients were placed in a supine position with the right hand at the most abducted position for right intercostal scanning. When at least 10 effective measurements were obtained with effective measurement at 60% or higher and interquartile range at less than 30%, such measurements were defined as effective and the median was employed as the result of the measurement.[20]

Analytical methods

In each group of liver diseases (HCV, HBV and NBNC), liver stiffness was compared between patients with and without HCC. Then, the cut-off value of liver stiffness for diagnosis of HCC was determined for later analysis in each group. Patients' backgrounds, laboratory data and liver stiffness in the HCV, HBV and NBNC groups were subjected to univariate, multivariate and subgroup analyses on the relationship with HCC. The 470 HCV patients without HCC at enrollment were followed up with the day of measurement of liver stiffness designated as day 0. Factors related to the development of HCC were examined by univariate and multivariate analyses using values for liver stiffness and blood test results at enrollment.

Statistical analysis

Category data were analyzed by the χ^2-test and Fisher's exact test, while numerical data were examined by Mann–Whitney *U*-test. The cut-off value was set to yield the largest Youden index by receiver–operator curve (ROC) analysis. Multiple logistic analysis was performed for multivariate analysis on factors related to HCC concurrence. The Cox regression hazard model was employed for multivariate analysis of factors related to HCC development. Yearly development of HCC was expressed as per person•year. Cumulative incidence of HCC development was calculated by the Kaplan–Meier curve. *P*-values less than 0.05 were considered significant.

RESULTS

Baseline characteristics

CLINICAL BACKGROUND FACTORS of 1002 patients were compared between patients with and without HCC according to group (Table 1). There were 722 cases in the HCV group, 104 in the HBV group and 176 in the NBNC group. For all groups there was a significant association with older age, low Alb and Plt,

Table 1 Baseline characteristics of patients with and without HCC

Factors	HCV patients ($n = 722$)			HBV patients ($n = 104$)			NBNC patients ($n = 176$)		
	HCC(+) ($n = 167$)	HCC(−) ($n = 555$)	P	HCC(+) ($n = 29$)	HCC(−) ($n = 75$)	P	HCC(+) ($n = 50$)	HCC(−) ($n = 126$)	P
Age (years)	72 (42–89)	61 (20–89)	<0.01	62 (49–76)	52 (19–73)	<0.01	70 (53–88)	63 (19–88)	<0.01
Sex (male/female)	111/56	288/266	<0.01	23/6	47/28	0.11	33/17	69/58	0.16
Alb (g/dL)	3.6 (1.8–5.1)	4.3 (2.1–5.3)	<0.01	4.4 (2.0–5.0)	4.5 (3.5–5.2)	0.04	3.8 (1.9–4.7)	4.1 (2.4–5.5)	<0.01
T-Bil (mg/dL)	0.8 (0.3–4.7)	0.7 (0.2–26.9)	<0.01	0.7 (0.3–1.2)	0.7 (0.2–1.6)	0.45	0.7 (0.1–1.5)	0.7 (0.1–2.3)	0.90
AST (U/L)	48 (13–340)	32 (8–262)	<0.01	28 (16–95)	25 (14–178)	0.06	43 (17–146)	32 (10–291)	0.03
ALT (U/L)	43 (4–557)	32 (2–334)	<0.01	25 (10–134)	21 (9–375)	0.13	29 (10–80)	29 (6–517)	0.99
γ-GT (U/L)	36 (11–918)	28 (9–354)	<0.01	56 (13–267)	21 (8–222)	<0.01	74 (15–628)	55 (7–743)	0.14
Plt (10^9/L)	94 (25–299)	157 (40–343)	<0.01	118 (21–207)	172.5 (58–300)	<0.01	117 (14–264)	168 (30–387)	<0.01
AFP (ng/mL)	12.9 (1.3–54 923)	3.6 (0.8–839)	<0.01	3.8 (1.3–22 421)	2.7 (1.1–70.9)	<0.01	5.8 (1.3–5194)	3.2 (0.8–25.3)	<0.01
Stiffness (kPa)	21.3 (3.9–75.0)	7.8 (3.0–72.0)	<0.01	9.2 (4.7–75.0)	5.6 (2.8–32.4)	<0.01	15.6 (3.3–75.0)	7.4 (2.8–66.4)	<0.01
Hx of IFN Tx (yes/no)	38/129	153/402	0.21	–	–	–	–	–	–
SVR/non-SVR	10/34	56/97	0.09	–	–	–	–	–	–
Tx of NA	–	–	–	16/13	34/41	0.37	–	–	–
HBV-DNA >4 log copies/mL	–	–	–	4/25	16/59	0.38	–	–	–

Values are expressed as the mean (range).

–, Not applicable; AFP, α-fetoprotein; Alb, albumin; ALT, alanine aminotransferase; AST, aspartate aminotransferase; HBV patients, HBs antigen positive patients; HCC, hepatocellular carcinoma; HCV patients, HCV antibody positive patients; Hx, history; IFN, interferon; NA, nucleoside analog; NBNC patients, HBs antigen negative and HCV antibody negative patients; Plt, platelet count; stiffness, liver stiffness; SVR, sustained virological response; T-Bil, total bilirubin; Tx, Treatment; γ-GT, γ-glutamyl transpeptidase.

and elevated AFP among those with HCC. The proportion of males was significantly higher among the HCC cases in the HCV group. Stiffness of the liver was significantly greater among the HCC cases in all groups.

Determining cut-off values related to HCC concurrence in each disease group

The cut-off value most related to HCC concurrence was determined by the ROC analysis in each disease group. It was set at more than 12.0 kPa (>12.0 kPa vs ≤12.0 kPa; odds ratio [OR], 14.7; $P < 0.001$) in the HCV group, at more than 8.5 kPa (>8.5 kPa vs ≤8.5 kPa; OR, 8.28; $P < 0.001$) in the HBV group and at more than 12.0 kPa (>12.0 kPa vs ≤12.0 kPa; OR, 4.67; $P < 0.001$) in the NBNC group (Fig. 1).

HCC concurrence-related factors

Hepatocellular carcinoma concurrence-related factors in the HCV group were examined. Univariate analysis revealed that age, sex, Alb, total bilirubin, aspartate aminotransferase (AST), γ-glutamyltransferase (γ-GT), Plt, AFP and liver stiffness of more than 12.0 kPa were significant factors (Table 2). With the significant factors extracted by univariate analysis, multivariate analysis was performed, and age, sex, Alb, Plt and liver stiffness of more than 12.0 kPa were independent factors (Table 3). Liver stiffness of more than 12.0 kPa was significant with an OR of 4.53 ($P < 0.001$).

Hepatitis C virus patients were categorized into two groups according to liver stiffness of 12.0 kPa or less, and more than 12.0 kPa, and HCC concurrence-related factors were examined in each group. Multivariate analysis extracted age, sex, Alb and AFP in the group with liver stiffness of 12.0 kPa or less as independent factors, and age, Alb and Plt in the group with liver stiffness of more than 12.0 kPa (Table 3).

In the HBV group, HCC concurrence-related factors were examined. Univariate analysis revealed that age, Alb, γ-GT, Plt, AFP and liver stiffness of more than 8.5 kPa were significant factors (Table 2), and multivariate analysis extracted age as an independent factor (OR, 1.12 [range, 1.04–1.21], $P < 0.004$) while low Plt tended to be associated with a high risk for HCC occurrence (OR, 0.99 [range, 0.98–1.00], $P = 0.08$) (data not shown). Subgroup analysis showed that liver stiffness of more than 8.5 kPa was a significant factor for HCC concurrence irrespective of age of more than 60 years or 60 years or less, and Plt less than 150×10^9/L or 150×10^9/L or more (Fig. 2).

Also examined were HCC concurrence-related factors in the NBNC group. Univariate analysis revealed that Alb, Plt, AFP and liver stiffness of more than 12.0 kPa

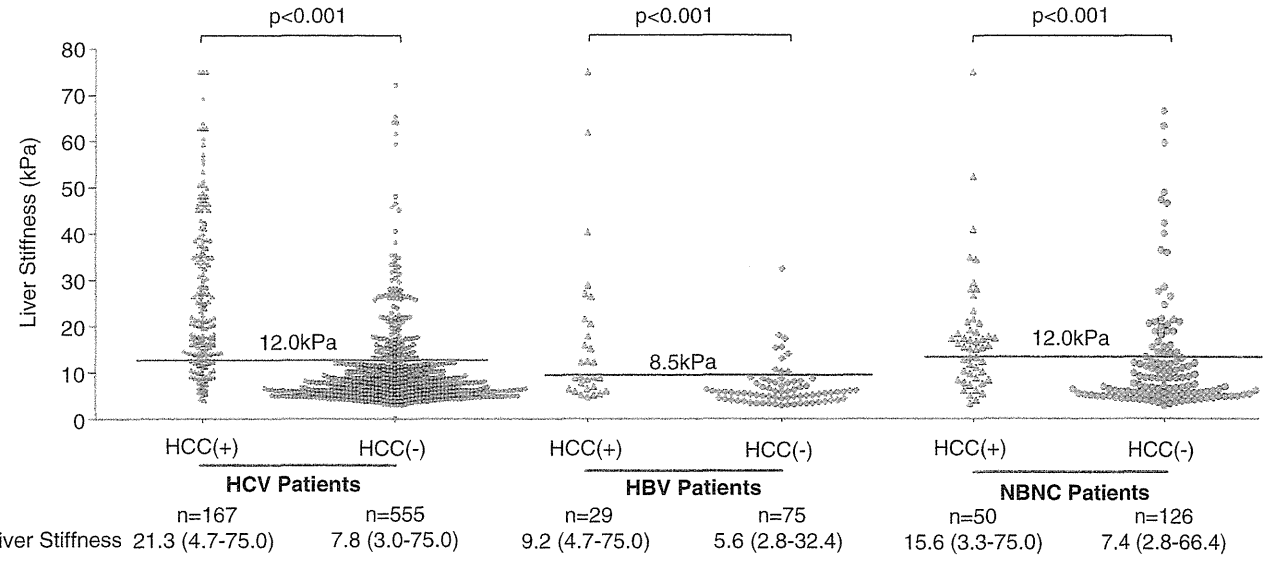

Figure 1 Distribution of liver stiffness categorized by the presence of hepatocellular carcinoma (HCC). Distribution of liver stiffness is shown in cases with liver disease of different etiologies with and without HCC. The cut-off value for liver stiffness was calculated so that sensitivity plus specificity would be the largest. A horizontal line indicating the cut-off value was drawn separately in each etiology group with an insertion of the value. Liver stiffness is shown as the median (range). Liver stiffness scores were significantly higher in cases with HCC concurrence. HBV, hepatitis B virus; HCV, hepatitis C virus; NBNC, non-B, non-C.

Table 2 Factors related to HCC: univariate analysis

Factors	HCV patients ($n = 722$)			HBV patients ($n = 104$)			NBNC patients ($n = 176$)		
	OR	95% CI	*P*	OR	95% CI	*P*	OR	95% CI	*P*
Age (years)	1.13	1.11–1.16	<0.001	1.09	1.04–1.14	<0.001	1.07	1.04–1.12	<0.001
Sex (male)	1.84	1.28–2.64	0.001	2.28	0.83–6.29	0.110	1.66	0.84–3.27	0.147
Alb (g/dL)	0.07	0.04–0.11	<0.001	0.20	0.07–0.59	0.003	0.33	0.17–0.63	<0.001
T-Bil (mg/dL)	1.53	1.09–2.14	0.014	1.20	0.24–6.02	0.826	0.80	0.32–2.03	0.639
AST (U/L)	1.01	1.01–1.02	<0.001	1.01	0.99–1.02	0.431	1.00	0.99–1.01	0.554
ALT (U/L)	1.00	0.99–1.01	0.103	0.99	0.99–1.01	0.868	0.99	0.98–1.00	0.281
γ-GT (U/L)	1.00	1.00–1.01	0.005	1.02	1.01–1.03	0.003	1.00	0.99–1.00	0.392
Plt (10^9/L)	0.98	0.97–0.98	<0.001	0.98	0.97–0.99	0.001	0.99	0.98–0.99	<0.001
AFP (ng/mL)	1.01	1.01–1.02	<0.001	1.04	1.00–1.08	0.033	1.14	1.04–1.26	0.007
Stiffness > cut-off value*	14.3	9.27–22.1	<0.001	7.13	2.76–18.4	<0.001	4.67	2.32–9.40	<0.001
Hx of IFN Tx (yes/no)	0.77	0.51–1.15	0.208	–	–	–	–	–	–
SVR patients	0.56	0.28–1.13	0.108	–	–	–	–	–	–
NA Tx	–	–	–	1.48	0.63–3.51	0.369	–	–	–
HBV DNA >4 log copies/mL	–	–	–	0.21	0.05–1.01	0.051	–	–	–

*The cut-off value is 8.5 kPa in HBV patients, and 12.0 kPa in HCV and NBNC patients.
–, Not applicable; AFP, α-fetoprotein; Alb, albumin; ALT, alanine aminotransferase; AST, aspartate aminotransferase; HBV patients, HBs antigen positive patients; HCC, hepatocellular carcinoma; HCV patients, HCV antibody positive patients; Hx, history; IFN, interferon; NA, nucleoside analog; NBNC patients, HBs antigen negative and HCV antibody negative patients; Plt, platelet count; stiffness, liver stiffness; SVR, sustained virological response; T-Bil, total bilirubin; Tx, Treatment; γ-GT, γ-glutamyl transpeptidase.

were significant factors (Table 2), and multivariate analysis extracted age and AFP as independent factors (data not shown). In the subgroup aged more than 65 years and AFP of less than 10 ng/mL, liver stiffness of more than 12.0 kPa was a significant HCC concurrence-related factor (Fig. 2).

Risk of HCC development in HCV infection

In the HCV group, the risk of HCC development was evaluated in 470 patients without HCC initially who were followed up. In contrast, evaluation of the risk of development of HCC was not possible in HBV or NBNC cases because no patient in those groups without HCC initially subsequently developed HCC during this limited observation period. These 470 HCV cases were categorized into those with liver stiffness of more than 12.0 kPa and 12.0 kPa or less based on the cut-off value determined at the analysis of HCC concurrence, and Kaplan–Meier curves for HCC occurrence were constructed. Five patients developed HCC over a median

Table 3 Factors related to HCC in HCV patients: multivariate analysis

Factors	All ($n = 722$)			≤12 kPa ($n = 460$)			>12 kPa ($n = 262$)		
	OR	95% CI	*P*	OR	95% CI	*P*	OR	95% CI	*P*
Age (years)	1.13	1.10–1.17	<0.001*	1.12	1.07–1.19	<0.001*	1.12	1.07–1.16	<0.001*
Sex (male)	3.55	1.98–6.39	<0.001*	43.4	4.88–387	<0.001*			
Alb (g/dL)	0.27	0.14–0.46	<0.001*	0.19	0.06–0.63	0.007*	0.29	0.14–0.61	0.001*
T-Bil (mg/dL)	1.21	0.66–2.22	0.526				1.02	0.52–2.02	0.946
AST (U/L)	1.00	0.99–1.00	0.419						
ALT (IU/L)							0.99	0.99–1.00	0.541
γ-GT (U/L)	1.00	0.99–1.01	0.285						
Plt (10^9/L)	0.99	0.98–0.99	0.008*	0.99	0.98–1.00	0.113	0.99	0.98–0.99	0.036*
AFP (ng/mL)	1.00	0.99–1.01	0.138	1.10	1.01–1.19	0.028*	1.00	0.99–1.01	0.159
Stiffness >12.0 kPa	4.53	2.36–8.69	<0.001*	–	–	–	–	–	–

*Statistically significant.
–, Not applicable; AFP, α-fetoprotein; Alb, albumin; ALT, alanine aminotransferase; AST, aspartate aminotransferase; CI, confidence interval; HCC, hepatocellular carcinoma; HCV, hepatitis C virus; IFN, interferon; NA, nucleoside analog; OR, odds ratio; Plt, platelet count; stiffness, liver stiffness; SVR, sustained virological response; T-Bil, total bilirubin; γ-GT, γ-glutamyl transpeptidase.

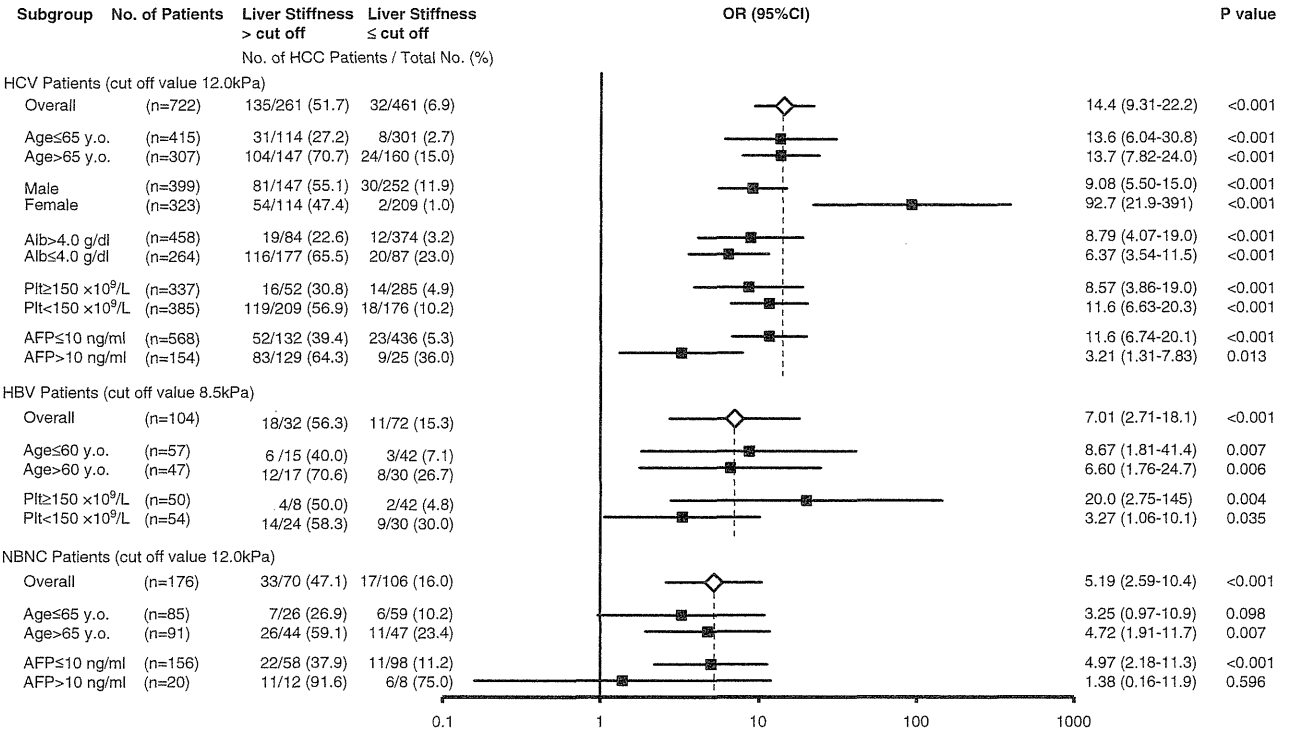

Figure 2 Odds ratio (OR) for the presence of hepatocellular carcinoma (HCC) in specified subgroups associated with liver stiffness over the cut-off value. The OR (95% confidence interval [CI]) for HCC and a *P*-value are shown for each subgroup of hepatitis C virus (HCV) patients with liver stiffness >12.0 kPa, hepatitis B virus (HBV) patients with liver stiffness >8.5 kPa and non-B, non-C (NBNC) liver disease patients with liver stiffness >12.0 kPa. Liver stiffness >12.0 kPa was a HCC concurrence-related factor in all subgroups of HCV patients. In particular, the association was stronger in females than in males. In HBV patients, liver stiffness >8.5 kPa was associated with HCC concurrence irrespective of age >60 years or ≤60 years and platelets (Plt) $\geq 150 \times 10^9$/L or $<150 \times 10^9$/L. In NBNC patients, liver stiffness >12.0 kPa was associated with HCC concurrence in the subcategory of age >65 years and α-fetoprotein (AFP) ≤10 ng/mL.

follow-up period of 691 days. The incidence of HCC development was significantly higher among cases with liver stiffness of more than 12.0 kPa than among those with liver stiffness of 12.0 kPa or less ($P < 0.001$, by log-rank test) (Fig. 3).

Factors related to HCC development were examined, and univariate analysis extracted elevated AST, elevated AFP and liver stiffness of more than 12.0 kPa as significant factors, and multivariate analysis revealed that liver stiffness of more than 12.0 kPa was an independent factor. A history of interferon treatment and a SVR were not independent risk factors (Table 4). Cumulative incidence of HCC development was 2.5% in 1 year and 6.1% in 2 years (2.63% per person•year) in patients with liver stiffness of more than 12 kPa. In those with liver stiffness of 12.0 kPa or less, it was 0% in 1 year and 0% in 2 years (0.15% per person•year).

DISCUSSION

WE FOUND THAT stiffness of the liver was significantly greater in those with HCC in the HCV, HBV and NBNC groups than among cases without HCC. In the HCV group, liver stiffness of more than 12.0 kPa was the most appropriate cut-off value for HCC concurrence producing the highest OR and the stiffness significantly correlated with HCC development. Likewise, liver stiffness of more than 8.5 kPa and more than 12.0 kPa were the most appropriate cut-off values associated with HCC concurrence in the HBV group and the NBNC group, respectively.

FibroScan has been widely used as a non-invasive measurement system for liver fibrosis. The most appropriate cut-off value for diagnosis of liver cirrhosis was 11.8–15.9 kPa with sensitivity ranging 79–87% and

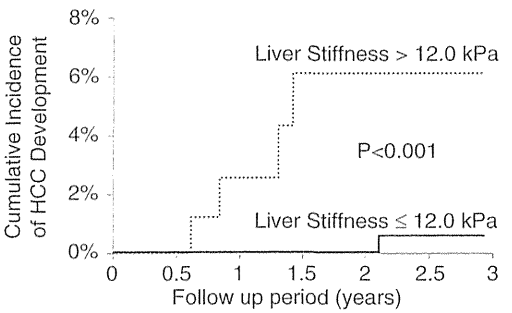

No. at risk

Liver Stiffness ≤ 12.0 kPa	366	326	278	248	175	122	50
Liver Stiffness > 12.0 kPa	104	85	69	52	36	19	10

Figure 3 Cumulative incidence of hepatocellular carcinoma (HCC) development in hepatitis C virus patients. Cumulative incidence of HCC development in cases with liver stiffness >12 kPa and ≤12 kPa is shown. Four and one case developed HCC among cases with liver stiffness >12 kPa and ≤12 kPa, respectively. Liver stiffness >12 kPa was associated with a significantly higher risk of HCC development than liver stiffness ≤12 kPa ($P < 0.001$). No case with liver stiffness ≤12 kPa developed HCC for at least 2 years.

specificity 81–95% in the HCV cases, 11.7 kPa with a sensitivity of 84.6% and specificity of 81.5% in the HBV cases,[17,21–23] and 10.3–17.5 kPa with sensitivity ranging 92–100% and specificity 88–97% in non-alcoholic fatty liver disease cases.[8,11,24] On the other hand, the value for liver stiffness most significantly related to HCC concurrence not to liver cirrhosis in each disease group remains elusive.[16,18,25]

The present analysis revealed that the cut-off value most closely associated with HCC concurrence was 12.0 kPa in the HCV group. Masuzaki *et al.* reported that HCC concurrence was more frequent in the presence of a firmer liver, but presented no appropriate cut-off value.[25] In contrast, Akima *et al.* and Kuo *et al.* reported that 12.5 kPa and 12.0 kPa were, respectively, the most appropriate cut-off values for HCC concurrence. However, their studies included heterogeneous etiologies and the cut-off level was not examined separately according to each etiology.[13,16] On the other hand, these cut-off values were almost comparable with the cut-off of 12.0 kPa in the present study because most cases in these studies were positive for HCV. The cut-off level for liver stiffness at 12.0 kPa, which was most closely associated with HCC concurrence in the present study, was almost comparable to the minimum cut-off level of liver stiffness for diagnosis of liver cirrhosis. In HCV positive cases, HCC concurrence was more frequent in cases with a histological semiquantitative diagnosis of fibrosis at F4 (liver cirrhosis) by liver biopsy.[6,26,27] These clinical observations were consistent with the quantitative results of the present study.

In the HCV group, liver stiffness of more than 12.0 kPa was associated with HCC concurrence independently of other factors associated with HCC concurrence, such as age, sex, Alb and Plt (Table 3). It has been reported that male sex and old age were risk factors for HCC independent of liver fibrosis.[6,28–30] Although it is presumed that low Alb and Plt are indirectly implicated in the advancement to liver cirrhosis, liver stiffness was independent of those factors and may reflect the risk for HCC directly related to fibrosis. Subgroup analysis (Fig. 2) revealed that liver stiffness of more than 12.0 kPa was more closely associated with HCC concurrence in females than in males. It was elucidated that HCC development was more closely associated with advancement of liver fibrosis in females and that measurement of liver stiffness in females was more useful than in males.

Although it is rare, some HCV positive cases develop HCC before clinical advancement to liver cirrhosis, and the clinical characteristics of such cases have been poorly investigated. To investigate HCC concurrence-related factors, we categorized HCV positive cases into two groups according to liver stiffness of more than 12.0 kPa and 12.0 kPa or less (Table 3). In those with mild liver fibrosis with liver stiffness of 12.0 kPa or less, old age, male sex, low Alb and elevated AFP were HCC concurrence-related factors. It was suggested that the risk of developing HCC was increased even in cases with mild liver fibrosis as long as those factors were present. Recently, it was reported that metabolic factors such as diabetes and non-alcoholic steatohepatitis are associated with HCC development independently of liver fibrosis.[31–33] It is necessary to further investigate how metabolic factors influence HCC development in patients with mild liver fibrosis and low values for measurements of liver stiffness.

Furthermore, in the HCV group, 470 cases without HCC were followed up (median, 691 days), and liver stiffness of more than 12.0 kPa was the only independent factor for HCC development (hazard ratio, 12.3; 95% confidence interval, 1.27–132) (Table 4). Curves for cumulative incidence of HCC development revealed that HCC development rates were significantly different between cases with liver stiffness of more than 12.0 kPa and 12.0 kPa or less ($P < 0.001$; log-rank test) and that HCC developed beginning 6 months after measurements in cases with liver stiffness of more than 12.0 kPa, whereas no HCC developed for at least 2 years in cases

Table 4 Factors related to HCC development in HCV patients

Factors	Patients who developed HCC $n = 5$	Patients who did not develop HCC $n = 465$	Univariate			Multivariate		
			HR	95% CI	*P*	HR	95% CI	*P*
Age (years)	60 (51–72)	61 (20–88)	1.01	0.93–1.10	0.837			
Sex (male)	4 (80.0%)	245 (52.7%)	4.49	0.50–40.3	0.180			
Alb (g/dL)	4.6 (3.4–4.8)	4.3 (2.1–5.3)	1.56	0.16–15.7	0.705			
T-Bil (mg/dL)	1.2 (0.5–2.4)	0.6 (0.2–26.9)	1.10	0.86–1.40	0.442			
AST (U/L)	84 (19–131)	32 (8–262)	1.02	1.00–1.03	0.013*	1.01	0.99–1.02	0.358
ALT (U/L)	49 (13–163)	31 (2–334)	1.01	0.99–1.02	0.179			
γ-GT (U/L)	51 (12–130)	28 (9–354)	1.01	0.99–1.02	0.223			
Plt (10^9/L)	98 (82–173)	156 (43–343)	0.98	0.97–1.00	0.128			
AFP (ng/mL)	6.2 (2.1–272.8)	3.5 (0.8–839)	1.00	1.00–1.01	0.025*	1.00	0.99–1.01	0.271
History of IFN	3 (60.0%)	256 (55.1%)	0.62	0.10–3.87	0.609			
SVR patients	1 (20.0%)	124 (26.7%)	0.38	0.04–3.45	0.388			
Stiffness >12.0 kPa	4 (80.0%)	103 (22.2%)	18.9	2.10–171	<0.001*	12.9	1.27–132	0.031*
Follow-up period (days)	477 (223–963)	691 (23–1069)	–	–	–	–	–	–

*Statistically significant.

Values are expressed as the mean (range) or *n* (%).

–, Not applicable; AFP, α-fetoprotein; Alb, albumin; ALT, alanine aminotransferase; AST, aspartate aminotransferase; CI, confidence interval; HCC, hepatocellular carcinoma; HCV, hepatitis C virus; HR, hazards ratio; IFN, interferon; NA, nucleoside analog; Plt, platelet count; stiffness, liver stiffness; SVR, sustained virological response; T-Bil, total bilirubin; γ-GT, γ-glutamyl transpeptidase.

with liver stiffness 12.0 kPa or less (Fig. 3). According to the HCC surveillance guidelines, an imaging examination every 6 months is recommended in cases with chronic hepatitis C and once in 3–4 months in cases with liver cirrhosis C.[34] In cases with liver stiffness of more than 12.0 kPa, the guidelines can be considered reasonable. In addition, in cases with liver stiffness of 12.0 kPa or less, it was suggested that the surveillance interval may be prolonged, although further accumulation of such cases was necessary.

In the HBV group, the cut-off value at 8.5 kPa most closely correlated with HCC concurrence (OR, 8.28), and both the cut-off value and OR were lower than those in the HCV group, which indicated that there was a weaker association between fibrosis and HCC in the HBV group than in the HCV group. In the HBV group, it was reported that liver stiffness at 8.0 kPa, a cut-off value lower than that in the HCV group, or higher increased the incidence of HCC development.[15] Subgroup analysis (Fig. 2) revealed that liver stiffness of more than 8.5 kPa was a significant factor irrespective of age and Plt. Unfortunately, we could not analyze the HCC developmental risk in cases with HBV because no case without concurrent HCC initially developed HCC during this limited observation period.

To the best of our knowledge, no report has demonstrated the association between liver stiffness and HCC concurrence in cases with NBNC liver disease, but when liver stiffness at 12.0 kPa was set as the cut-off value, liver stiffness most closely correlated with HCC concurrence and the cut-off value was almost comparable to that in the HCV group. This result demonstrates that fibrosis also plays an important role in HCC development in NBNC though its contribution is weaker than in HCV. Subgroup analysis revealed that HCC concurrence was more frequent in the group with liver stiffness of more than 12.0 kPa among the elderly aged more than 65 years old and cases with low AFP levels as reported previously,[32] demonstrating that the HCC risk was more greatly dependent on fibrosis in the elderly, while it was high irrespective of fibrosis in cases with elevated AFP in the NBNC group. As for etiologies in the NBNC group, most cases were clinically suspected to have fatty liver-associated diseases. Though information on steatosis-related factors was available only from limited cases in this study, high hemoglobin A1c (HbA1c) value (defined as >6.5) was frequent in NBNC cases (25%) compared to HCV (11%) or HBV cases (17%), and this difference reached statistical significance between HCV and NBNC (data not shown). In addition, high HbA1c value and heavy alcohol intake of more than 70 g/day were more significantly identified in HCC cases compared to non-HCC cases in the NBNC group (data not shown). These observations suggested that fatty liver-associated diseases may be one of the main etiologies in the NBNC group. On the other hand, as with the HBV cases, we could not analyze the HCC developmental risk in cases with NBNC because no case developed HCC during this limited observation period.

In conclusion, evaluation of liver fibrosis based on liver stiffness was useful, in particular, in HCV and NBNC liver disease, because HCC development via advancement of liver fibrosis is a major pathway. Accurate evaluation of liver fibrosis would be important to screen the high risk group for HCC development and analyze causal factors for HCC development other than fibrosis.

REFERENCES

1 Jemal A, Bray F, Center MM, Ferlay J, Ward E, Forman D. Global cancer statistics. *CA Cancer J Clin* 2011; **61** (2): 69–90.
2 El-Serag HB. Hepatocellular carcinoma. *N Engl J Med* 2011; **365** (12): 1118–27.
3 Ikeda K, Saitoh S, Suzuki Y *et al.* Disease progression and hepatocellular carcinogenesis in patients with chronic viral hepatitis: a prospective observation of 2215 patients. *J Hepatol* 1998; **28** (6): 930–8.
4 Inoue A, Tsukuma H, Oshima A *et al.* Effectiveness of interferon therapy for reducing the incidence of hepatocellular carcinoma among patients with type C chronic hepatitis. *J Epidemiol* 2000; **10** (4): 234–40.
5 Takano S, Yokosuka O, Imazeki F, Tagawa M, Omata M. Incidence of hepatocellular carcinoma in chronic hepatitis B and C: a prospective study of 251 patients. *Hepatology* 1995; **21** (3): 650–5.
6 Yoshida H, Shiratori Y, Moriyama M *et al.* Interferon therapy reduces the risk for hepatocellular carcinoma: national surveillance program of cirrhotic and noncirrhotic patients with chronic hepatitis C in Japan. IHIT Study Group. Inhibition of Hepatocarcinogenesis by Interferon Therapy. *Ann Intern Med* 1999; **131** (3): 174–81.
7 Sandrin L, Fourquet B, Hasquenoph JM *et al.* Transient elastography: a new noninvasive method for assessment of hepatic fibrosis. *Ultrasound Med Biol* 2003; **29** (12): 1705–13.
8 Abenavoli L, Beaugrand M. Transient elastography in non-alcoholic fatty liver disease. *Ann Hepatol* 2012; **11** (2): 172–8.
9 Cardoso AC, Carvalho-Filho RJ, Marcellin P. Transient elastography in chronic viral hepatitis: a critical appraisal. *Gut* 2011; **60** (6): 759–64.
10 Castera L. Non-invasive assessment of liver fibrosis in chronic hepatitis C. *Hepatol Int* 2011; **5** (2): 625–34.